

NASA CR 116772
N71-23250

HIGH TOTAL TEMPERATURE SENSING PROBE
FOR THE X-15 HYPERSONIC AIRCRAFT

**CASE FILE
COPY**

12080-FRI

Distribution of this report is provided in the interest of
information exchange. Responsibility for the contents
resides in the author or organization that prepared it.

SEPTEMBER 1968

Prepared under Contract No. NAS4-1211 by

HONEYWELL INC.
Systems & Research Division
Minneapolis, Minn.

for

NATIONAL AERONAUTICS AND SPACE ADMINISTRATION

HIGH TOTAL TEMPERATURE SENSING PROBE
FOR THE X-15 HYPERSONIC AIRCRAFT

Ronald G. Bailey

September 1968

Distribution of this report is provided in the interest of information exchange. Responsibility for the contents resides in the author or organization that prepared it.

Prepared under Contract No. NAS4-1211 by
HONEYWELL INC.
Systems and Research Division
Minneapolis, Minnesota

for

Flight Research Center
NATIONAL AERONAUTICS AND SPACE ADMINISTRATION

FOREWORD AND ACKNOWLEDGEMENT

This final report describes the work accomplished by Honeywell Inc. for the Instrument Development Branch, Data Systems Division, at NASA Flight Research Center in accordance with the requirements defined by Contract NAS4-1211, entitled, "High Total Temperature Sensing Probe for the X-15 Hypersonic Aircraft." This report has been prepared to fulfill the requirements of Article III of the subject contract.

The author wishes to acknowledge the guidance afforded by Mr. Rodney K. Bogue and Mr. Donald W. Veatch who monitored this work.

CONTENTS

	Page
SUMMARY	1
SYMBOLS	2
SUBSCRIPTS	4
GENERAL FLUID TECHNOLOGY	4
Proportional Amplifier	5
Fluid Oscillator	5
Fluid Temperature Sensing	6
COOLED SENSOR CONCEPT	6
INLET CONDITIONS	10
SENSOR OPERATION	14
SENSOR DESIGN	20
Probe Size Determination	21
Rounded Splitter	22
Sensor Flow	23
Preliminary Temperature Tests	28
MATERIAL SELECTION	31
FABRICATION	33
PROBE SYSTEM	34
Coolant System	37
Readout Electronics	38
TEMPERATURE TESTS AND CALIBRATION	44
Low-Temperature Tests	44
High-Temperature Test Facility	46
High-Temperature Tests	53
ENVIRONMENTAL REQUIREMENTS	67
TESTS ON THE X-15 AIRCRAFT	68
CONCLUSIONS	68

	Page
REFERENCES	71
APPENDIX A -- HIGH- AND LOW-TEMPERATURE DATA	
APPENDIX B -- ELECTRONIC COMPONENT SPECIFICATIONS	

ILLUSTRATIONS

Figure		Page
1	Cooled Sensor Schematic	8
2	Sensor Cooling Configuration	9
3	Cooled Sensor Flow Schematic	11
4	Altitude-Velocity Profile Envelope	12
5	Total Pressure-Altitude Envelope	13
6	Typical Profile Time History for Total Temperature	15
7	Typical Profile Time History for Total Pressure	16
8	Three Fluidic Temperature Sensing Probes	17
9	Fluidic Temperature Probe Schematic	18
10	Drag Coefficient versus Mach Number	21
11	Fluid Oscillator Splitter Temperature Distribution	24
12	Base Pressure-Inlet Pressure Ratio versus Free-Stream Mach Number	25
13	Oscillation Frequency versus Inlet Total Pressure In Air	27
14	Temperature Controlled Test Chamber	29
15	Experimental Cooled Sensor, Model Number Four	30
16	Shear Specimen Fixture, Assembled	35
17	Shear Specimen Fixture, Disassembled	35
18	Assembled and Disassembled Probe	36
19	Schematic of Coolant System	38
20	Coolant Flow Rate versus Inlet Temperature, Inlet Total Pressure = 3.0 in. Hg _{ABS}	39
21	Coolant Flow Rate versus Inlet Temperature, Inlet Total Pressure = 9.0 in. Hg _{ABS}	39

Figure		Page
22	Coolant Flow Rate versus Inlet Temperature, Inlet Total Pressure = 19.0 in. Hg _{ABS}	40
23	Coolant Flow Rate versus Inlet Temperature, Inlet Total Pressure = 29.0 in. Hg _{ABS}	40
24	Schematic of the Electronic Readout Circuit	42
25	Output Voltage versus Frequency	43
26	Three Electronic Readout Packages	43
27	Electronic Package Sketch	44
28	Prototype Fluidic Temperature Probe	45
29	Temperature Box and Test Equipment	45
30	STOKES Resistance Furnace - Outside View	47
31	STOKES Resistance Furnace - Inside View	47
32	Schematic of High-Temperature Calibration Setup	49
33	Temperature Probe Ready for Test	50
34	Temperature - Millivolt Equivalent for a Tungsten - 5 Percent Rhenium versus Tungsten - 26 Percent Rhenium Thermocouple	52
35	Typical Sensor Body Temperature Profiles	54
36	Body Temperature versus Oscillation Frequency for Air, Inlet Total Pressure = 3.0 in. Hg _{ABS}	56
37	Body Temperature versus Oscillation Frequency for Air, Inlet Total Pressure = 9.0 in. Hg _{ABS}	57
38	Body Temperature versus Oscillation Frequency for Air, Inlet Total Pressure = 19.0 in. Hg _{ABS}	58
39	Body Temperature versus Oscillation Frequency for Air, Inlet Total Pressure = 29.0 in. Hg _{ABS}	59
40	Inlet Temperature versus Oscillation Frequency for Air, Inlet Total Pressure = 3.0 in. Hg _{ABS}	60

Figure		Page
41	Inlet Temperature versus Oscillation Frequency for Air, Inlet Total Pressure = 9.0 in. Hg _{ABS}	61
42	Inlet Temperature versus Oscillation Frequency for Air, Inlet Total Pressure = 19.0 in. Hg _{ABS}	62
43	Inlet Temperature versus Oscillation Frequency for Air, Inlet Total Pressure = 29.0 in. Hg _{ABS}	63
44	Oscillation Frequency versus Inlet Total Pressure for Air	65
45	Oscillation Frequency versus Cavity Temperature for Air	66
46	Hypersonic Wind Tunnel Fluidic Temperature Probe	69

TABLES

Table		Page
1	Material Characteristics	32
2	Diffusion Bond Test Results	34
A1	High-Temperature Data	A2
A2	Low-Temperature Data	A3

SUMMARY

This document summarizes the work accomplished during a one-year study and hardware development effort by Honeywell Inc. Systems and Research Center on NASA Contract NAS4-1211, "High Total Temperature Sensing Probe for the X-15 Hypersonic Aircraft."

The ability of fluidic devices to sense and to control has brought to light many new applications for this broad new technology. This work applies the fluid oscillator concept to the development of a probe for measuring free-stream total temperatures on hypersonic aircraft of the X-15 class.

The probe generates an oscillating pressure signal in the form of a sonic pressure wave which is propagated and reflected within the device to cause an oscillation of the incoming fluid. The sensor oscillation frequency is dependent on the acoustical velocity of the wave within the fluid, and thus a function of the fluid temperature in the probe cavity.

The probe utilizes a cooled sensor concept in which the probe body temperature is maintained below the material melting point with nitrogen gas coolant. The free-stream total temperature is arrived at through measurements of the oscillation frequency, body temperature and local pitot pressure. The frequency is measured with two conventional pressure transducers arranged to operate in push-pull, with either transducer capable of independent operation should the other fail.

The time response of the instrument is dependent upon the purging time of the fluid within the sensor cavities which is about 10 milliseconds.

This fluid temperature measurement concept depends upon the dynamic flow of a gas and therefore requires that a differential pressure be developed across the sensor. This differential pressure is created by exhausting the sensor operating gas into the low-pressure base region of the probe.

The purpose of the study was to develop the cooled fluidic oscillator temperature sensor concept into working hardware of a size and design which would be compatible with mounting and operation on the X-15 aircraft.

Prior to contract initiation the fluidic temperature sensing method has been applied to the development of a probe for measuring high stagnation temperatures in high Mach fluid streams within NASA-Ames hypersonic wind tunnels. In October 1967, a miniature wind tunnel probe flew on the X-15 aircraft and successfully measured free-stream total temperatures ranging to 3350°R. Interest grew in utilizing this type of temperature measurement in the development of a probe designed specifically for X-15-type aircraft.

The probes and associated electronic readout equipment developed on Contract NAS4-1211 were designed to meet the rigid environmental conditions encountered by high-performance aircraft of the X-15 type. The probe is capable of measuring free-stream total temperatures ranging from 500°R to 5000°R at total pressures of 0.5 psia to 30 psia with repeatability within ± 2 percent of reading.

SYMBOLS

A	Sensor internal wetted area
\dot{c}	Coolant flow rate
C_p	Specific heat at constant pressure
C_{p_B}	Base pressure coefficient
f	Oscillation frequency
h	Heat transfer coefficient

k	Constant
k_T	Thermal conductivity
L	Characteristic length
m	Gas molecular weight
M	Mach number
\dot{m}	Sensor gas flow rate
n	Frequency exponent
N_u	Nusselt number
P	Total pressure
P_r	Prandtl number
q	Dynamic pressure
R	Gas constant
\mathcal{R}	Universal gas constant
R_e	Reynolds number
T	Temperature
γ	Ratio of specific heats
λ	Oscillator path length

SUBSCRIPTS

A	Air
b	Body
B	Base of sensor
c	Cavity
i	Inlet
∞	Free-stream

GENERAL FLUID TECHNOLOGY

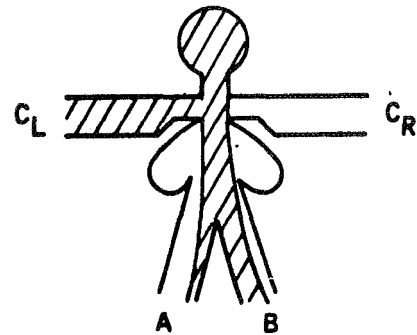
Because this work presents a new method of temperature sensing through the use of fluid techniques, we will digress momentarily to some basic fluid concepts.

A fluid amplifier is a high-energy stream of fluid modulated by a lower energy stream. It is an amplifier in the same sense that a cathode ray tube is an amplifier; i. e. , a high-energy stream of electrons is modulated by a lower powered electrostatic field near the base of the tube. For this analogy, the fluid amplifiers are often called beam-deflection-type amplifiers. There are other types of fluid amplifiers which do not use the beam deflection principle, but they are not appropriate to this discussion of temperature sensing techniques.

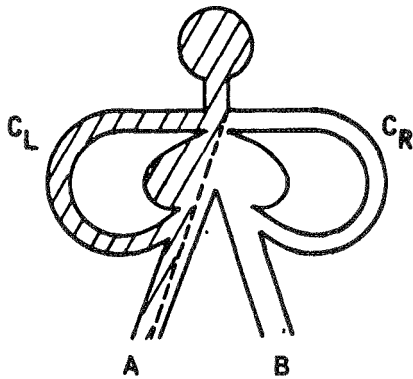
Proportional Amplifier

A basic member of the fluid amplifier family is the two-dimensional proportional fluid amplifier. As the name implies, it proportionately divides the inlet flow between two outlets depending upon control port (C_L and C_R) pressure.

Differential pressure applied by the control ports to the power stream produces a curvature in the stream such that it divides upon a downstream splitter in proportion to the applied differential pressure. In the amplifier at right, the left control port has the greater pressure, therefore curving the power stream so that the major proportion exits from leg B.



Fluid Oscillator



An oscillator may be constructed by taking some of the output flow of an amplifier and returning it to the control ports. At left some of the flow from leg A is being diverted to control port C_L which will force the fluid jet out leg B. Once the flow is established in leg B, part of it will be diverted to control port C_R to return the jet to the original position and the cycle will start over again.

As the fluid jet in an oscillator moves back and forth it generates acoustic signals in the output legs. These acoustic signals may be propagated through the return lines to the jet. Proper design will cause these acoustic signals to switch the jet rather than the fluid flow. The frequency of oscillation then is a function of the propagation path length and the acoustic velocity.

Fluid Temperature Sensing

Recent advances in fluid technology have shown new ways to use fluid devices to compute and to sense. In particular, a fluid oscillator, similar in principle to the one described in the foregoing paragraphs, exhibits the ability to sense the temperature of the operating gas.

The oscillator consists of a submerged fluid jet which is forced to oscillate back and forth by an acoustically propagated pressure front generated within the device. The acoustic velocity of the pressure front and its path length determine the cycle time and thus the oscillation frequency of the sensor. For a given geometry sensor operating with adequate flow, the acoustic path length remains constant and therefore the output frequency is a function of the acoustic velocity only. This may be expressed for steady-state conditions as $f = k \sqrt{\gamma RT}$ where k is an instrument calibration constant, γ is the ratio of specific heats of the operating gas ($C_p/C_v = 1.4$ for air), R is the gas constant ($1716 \text{ ft}^2/\text{sec}^2 \text{ }^\circ\text{R}$ for air) and T is the absolute temperature of the sensor cavities and quite close to inlet stagnation temperature because of the low fluid velocities in the cavity.

The temperature-sensitive oscillator has a unique capability in the field of high-temperature fluid measurements in that its range of temperature application is a function only of the material used in its fabrication and whether the sensor is cooled. See COOLED SENSOR CONCEPT section. Moreover, the material utilized does not, for the most part, affect operation of the oscillator; hence, structural integrity is the only criterion in its selection.

COOLED SENSOR CONCEPT

As it becomes necessary to measure higher and higher gas temperatures, the requirement for a sensor material becomes more severe and the selection

more limited. Ceramic materials are candidates for applications involving slow temperature changes where thermal shock is not a problem. The refractory metals are capable of being exposed to very high temperatures in nonoxidizing atmospheres only.

In cases where a temperature or transducer probe measurement is desired in air above 3500°R, heat and oxidation problems are critical unless probe cooling is provided. In the case of the thermocouple, cooling reduces the junction temperature and produces an incorrect reading. This can be corrected only with a rather complex set of heat balance equations which must take into account conductive effects (from the cooling medium) as well as radiation and convective effects.

These corrections are additionally difficult to compute because the temperature of the body to which radiation occurs is not known and fluid density variations (with altitude and temperature) make the input heat rate difficult to determine. For this reason, thermocouple techniques usually rely upon large massive junctions, which slowly ablate away for protection from the extreme heat. These devices have inherently poor time response.

An advantage of the cooled fluid temperature sensor is that the body temperature may be kept to a reasonable value while the working gas temperature remains high. The fluidic temperature sensor measures the temperature of the fluid sample by the velocity of an acoustic propagation within the sensor passages. If the sensor is externally cooled, the fluid sample will be cooled by the cooler sensor walls. However, no external radiation effects are present, and the acoustically-measured temperature may be related to the inlet fluid temperature by an analytical function containing the sensor body temperature. Body temperature is, of course, easy to measure with thermocouple techniques because it is relatively cool.

To a first-order approximation we assume the sensor to be similar to an open pipe for heat transfer considerations (Figure 1).

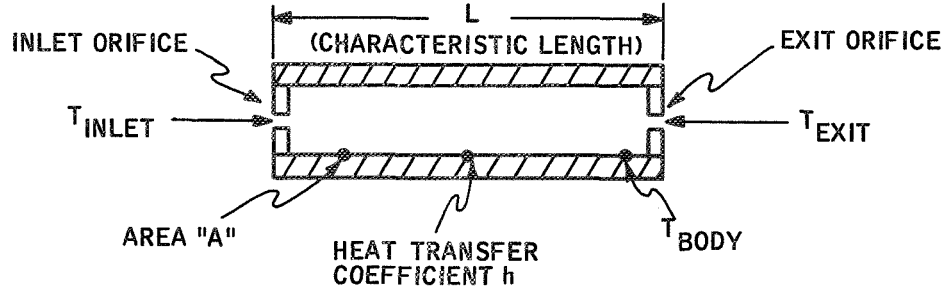


Figure 1. Cooled Sensor Schematic

Now if the inlet and exit pressures remain relatively constant, then the Nusselt number,

$$N_u = \frac{hL}{k_T} = \xi(R_e, P_r, M), \quad k_T \text{ is thermal conductivity,}$$

will remain constant and the heat transfer coefficient, h , will be a constant. We then may write a simple heat balance:

$$2\dot{m}C_p (T_i - T_c) = Q = h A (T_c - T_b)$$

$$T_i = \left(\frac{hA}{2\dot{m}C_p} \right) (T_c - T_b) + T_c$$

The steady-state frequency output of the fluid temperature sensor may be related to the absolute temperature of the gas in the cavity by the relation $f = k \sqrt{\gamma R T_c}$, as previously stated. When used as a temperature sensor, it is of more value to express an inverse function where the measured temperature is the dependent variable, such as

$$T_c = \frac{k_1 f^n}{\gamma R}$$

Let

$$\frac{hA}{2\dot{m}C_p} = k_2$$

then

$$T_i = -k_2 T_b + (1 + k_2) \left(\frac{f_{k1}^n}{\gamma R} \right)$$

The absolute temperature of the inlet fluid to the temperature sensor may then be expressed as:

$$T_i = (1 + k_2) \left(\frac{f_{k1}^n}{\gamma R} \right) - k_2 T_b$$

The concept of cooling the sensor requires that top and bottom manifolds be placed on the basic sensor configuration and coolant passages be provided in the sensor body (Figure 2). The measurement of sensor body temperatures

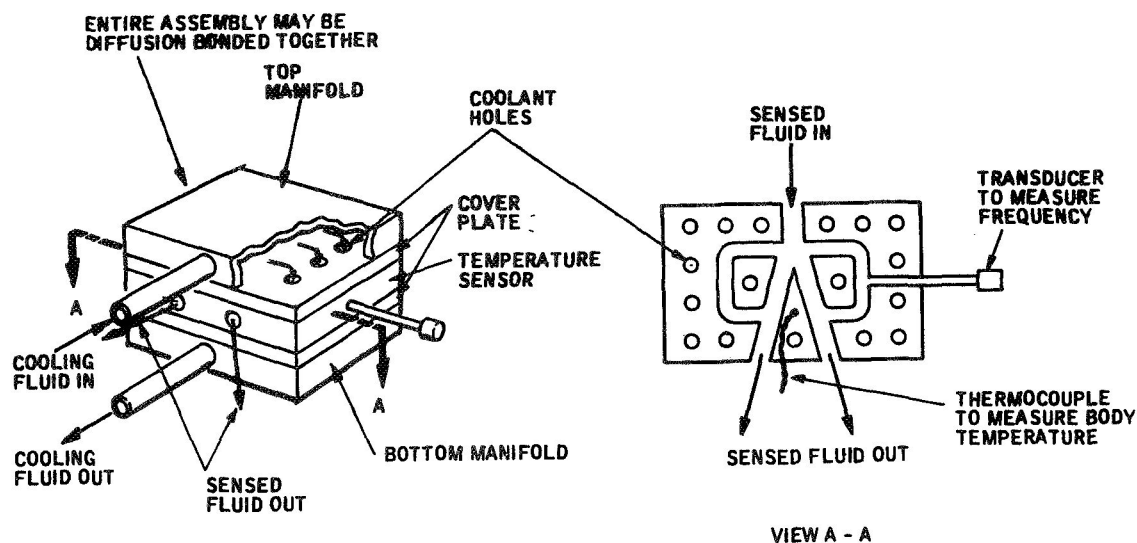


Figure 2. Sensor Cooling Configuration

may be obtained at some convenient place with a common thermocouple. Because temperature of the body is measured and corrected for, no control is necessary for the cooling fluid other than to provide a supply sufficient to avoid melting the sensor.

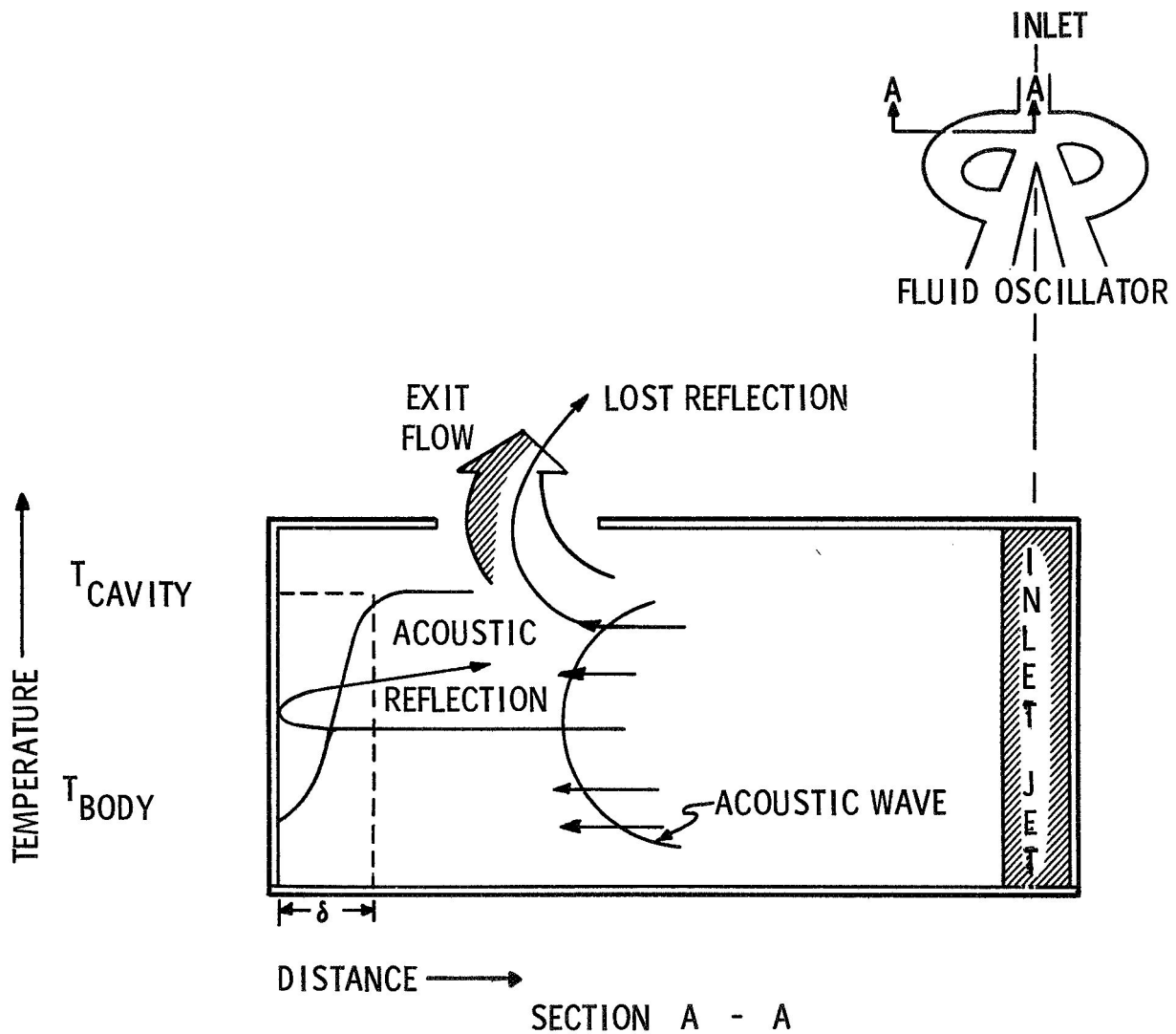
The mechanics of the flow and acoustic wave propagation within a cooled oscillator temperature sensor are shown in Figure 3. Because the oscillator body is cooler than the cavity gas, the gas near the wall is cooled by the wall, resulting in boundary layer flow with a steep temperature gradient. In actual sensor operation, the flow leaving the oscillator cavity comes from the boundary layer. This cooled gas is continually dumped, thereby insulating the hotter cavity gas which supports the acoustic wave propagation. It is important to point out that the time required for the acoustic reflection to traverse the boundary layer is very small. Therefore, the lower temperature of the boundary layer gas has little effect on the acoustic wave velocity.

INLET CONDITIONS

The primary goal of the contract was to develop a sensor which would be capable of accurately measuring free-stream total temperature over a flight envelope which is characteristic of vehicles in the X-15 aircraft class. As indicated on the altitude-velocity profile envelope, Figure 4, temperatures range to about 5300°R.

From Figure 4 and with the aid of Reference 1 a range of pitot pressures (sensor inlet total pressure) was determined. Refer to Figure 5. The values varied from about 2.5 psia occurring at 120,000 feet to about 31 psia at 85,000 feet.

The calculated pressures assume no aircraft shock wave effects. If at supersonic speeds the X-15 airplane is completely within the Mach cone generated at the nose of the aircraft, any total pressure or total temperature



δ = BOUNDARY LAYER THICKNESS

Figure 3. Cooled Sensor Flow Schematic

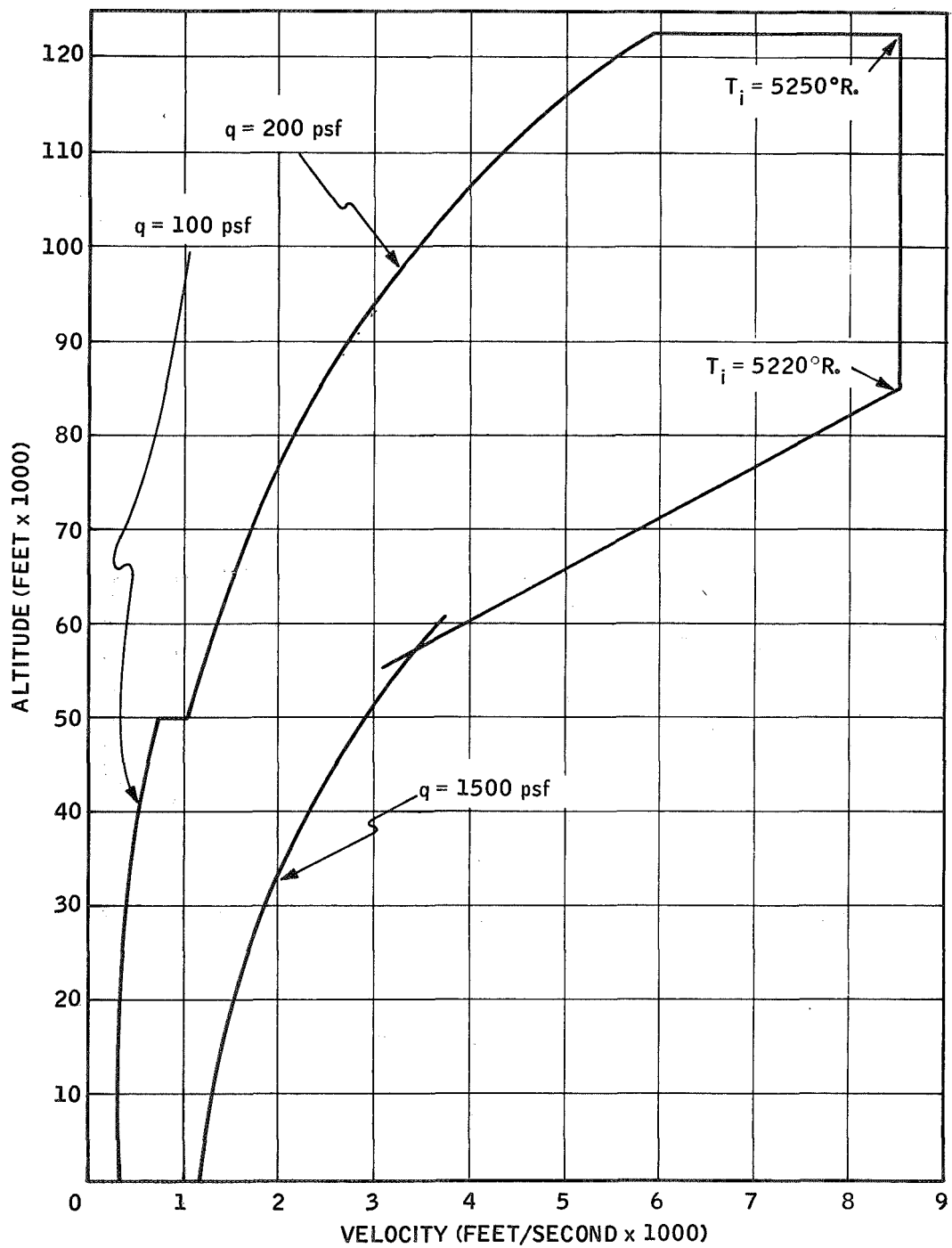


Figure 4. Altitude-Velocity Profile Envelope

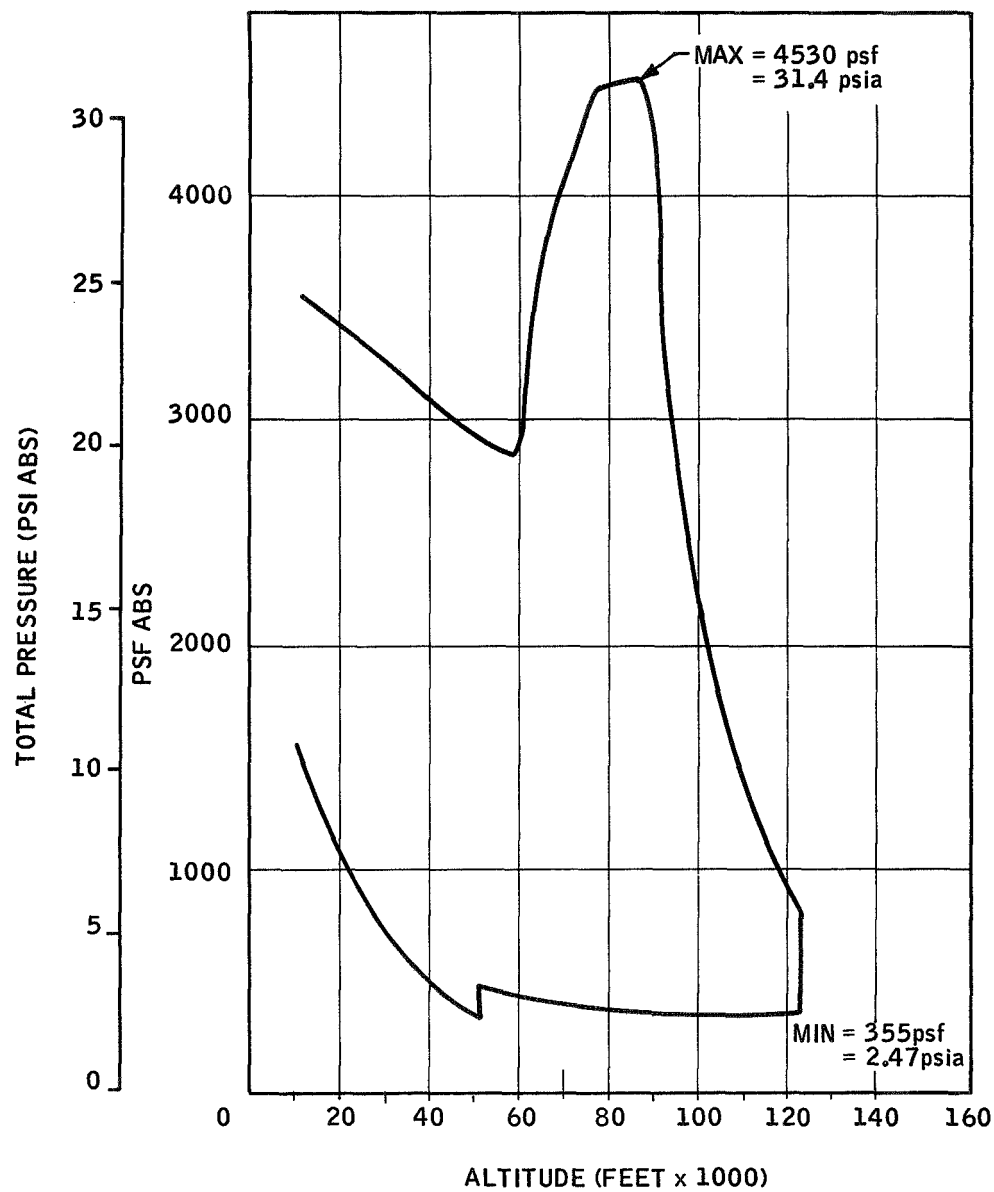


Figure 5. Total Pressure-Altitude Envelope

sensing instrument on the surface of the aircraft would have to be calibrated and corrected for Mach number, altitude and fuselage location. Once these corrections are applied, the instrument can be used to accurately sense stagnation temperatures during free flight.

Typical profile time histories for total temperature and total pressure are shown in Figures 6 and 7.

SENSOR OPERATION

The temperature probes developed on NASA Contract NAS4-1211, shown in Figure 8, will accurately measure free-stream total temperature on a vehicle in the X-15 class. The sensor will function reliably in environments which are normally encountered by high-performance aerospace vehicles which operate inside the atmosphere. Specifically, the sensor is capable of measuring total temperature over a range 500°R to 5000°R with an accuracy of better than ± 2 percent of reading. The sensor will produce a readable signal at inlet pressures ranging from 0.5 psia to 30 psia.

The temperature probe designed to meet these requirements is based on a fluidic temperature sensing concept. The sensor which samples the free-stream air consists of a fluid oscillator that generates an oscillating pressure wave within itself. The frequency of the oscillation is a function of the acoustical velocity of the pressure wave and therefore a function of the fluid temperature.

The fluidic oscillator assembly developed for the X-15 temperature probe measures about 1.4 in. wide by 0.4 in. high by 2.5 in. deep. This oscillator assembly is supported (welded) atop a pylon which can be easily held in a mounting fixture. The oscillator assembly and pylon are shown schematically in Figure 9.

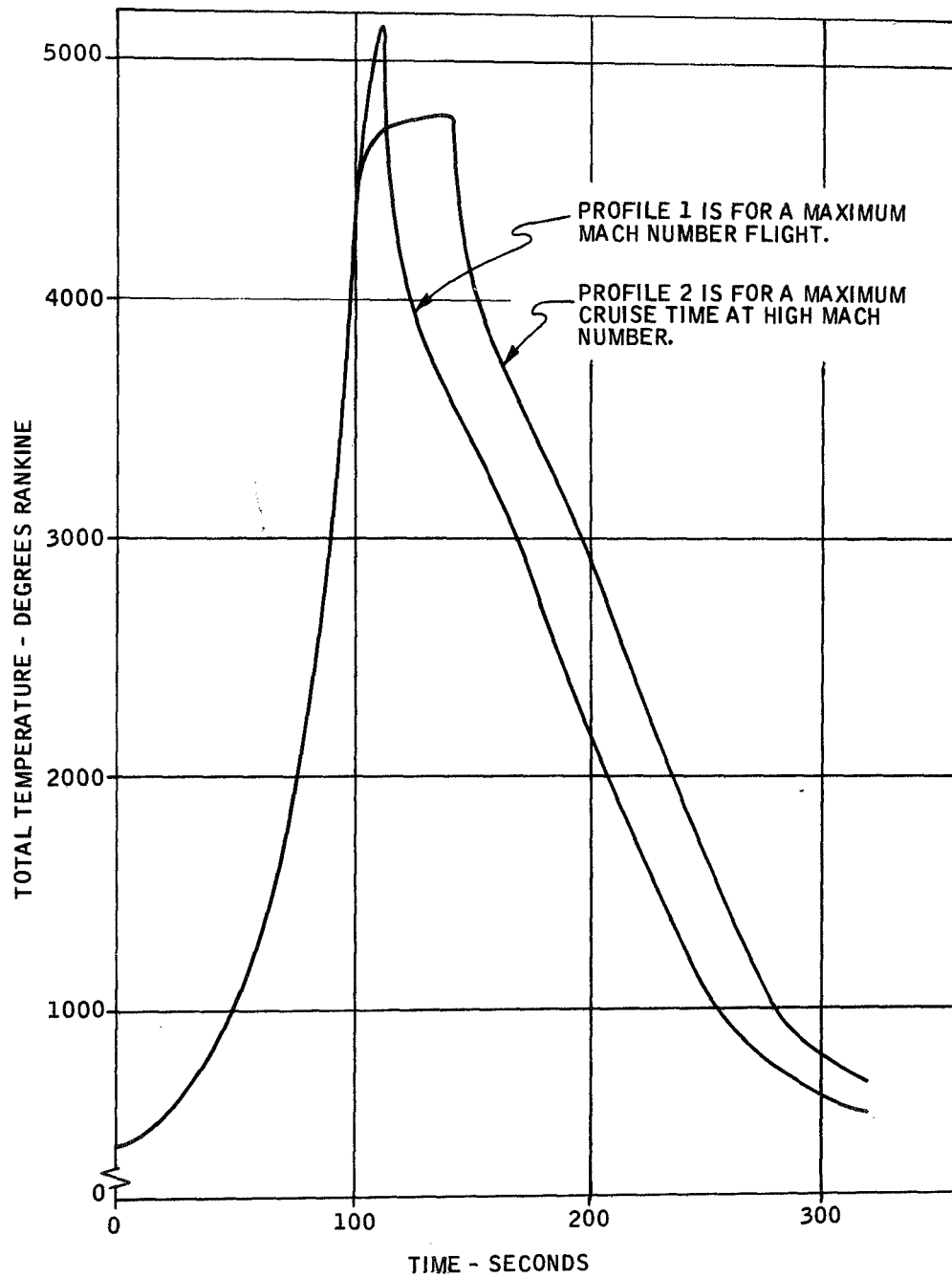


Figure 6. Typical Profile Time History for Total Temperature

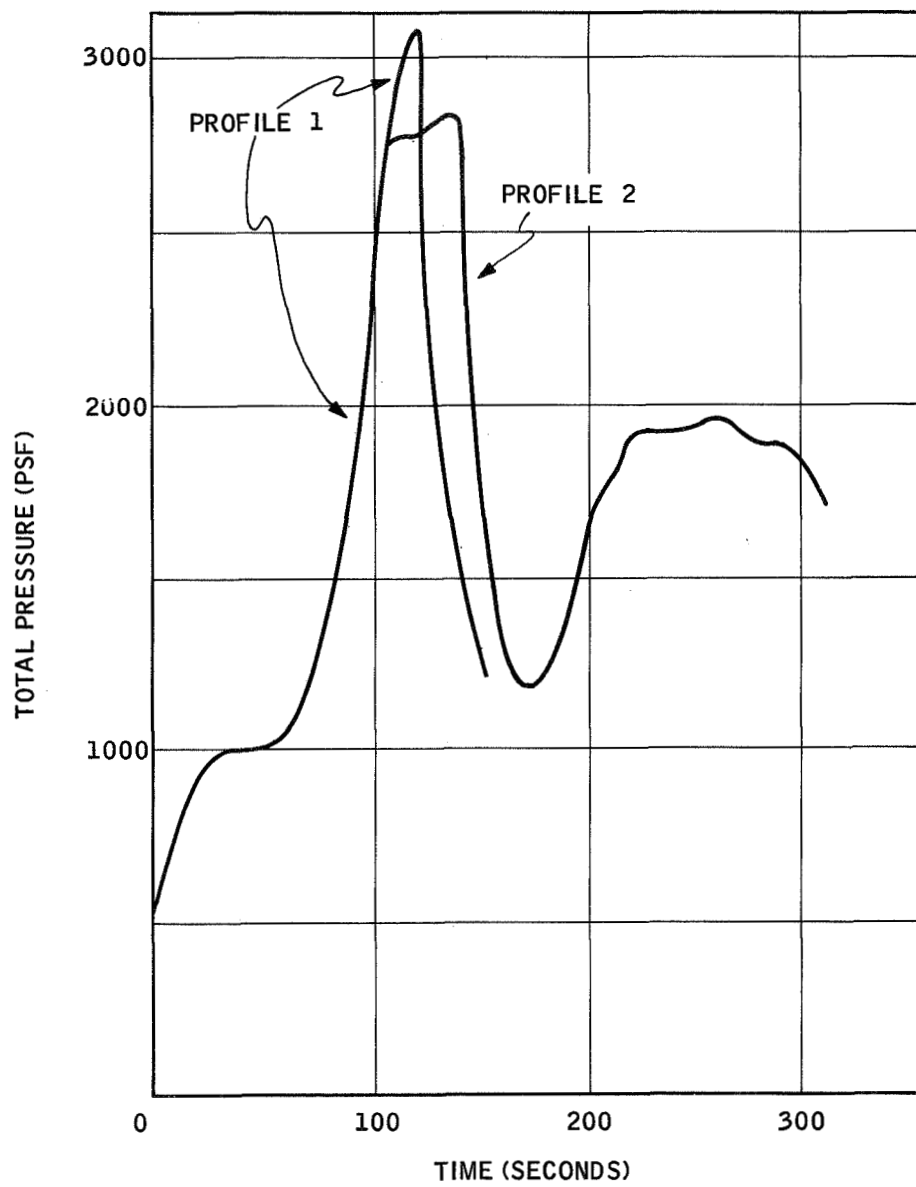


Figure 7. Typical Profile Time History for Total Pressure

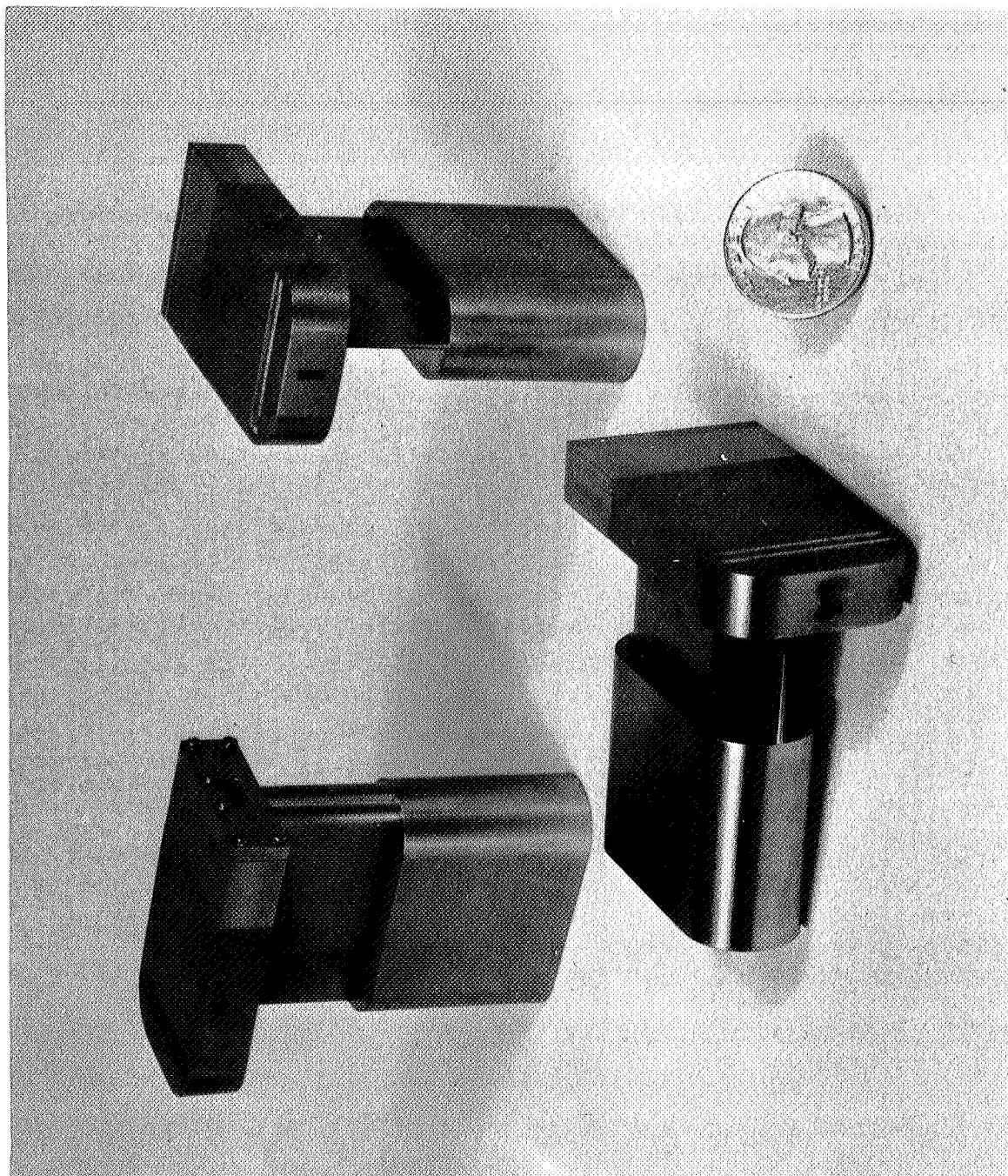




Figure 8. Three Fluidic Temperature Sensing Probes

NOTES:
1-MATERIAL: STAINLESS STEEL 446

FLOW KEY
 GAS FLOW
 COOLANT FLOW

0 0.25 0.5 0.75 1.0
SCALE IN INCHES

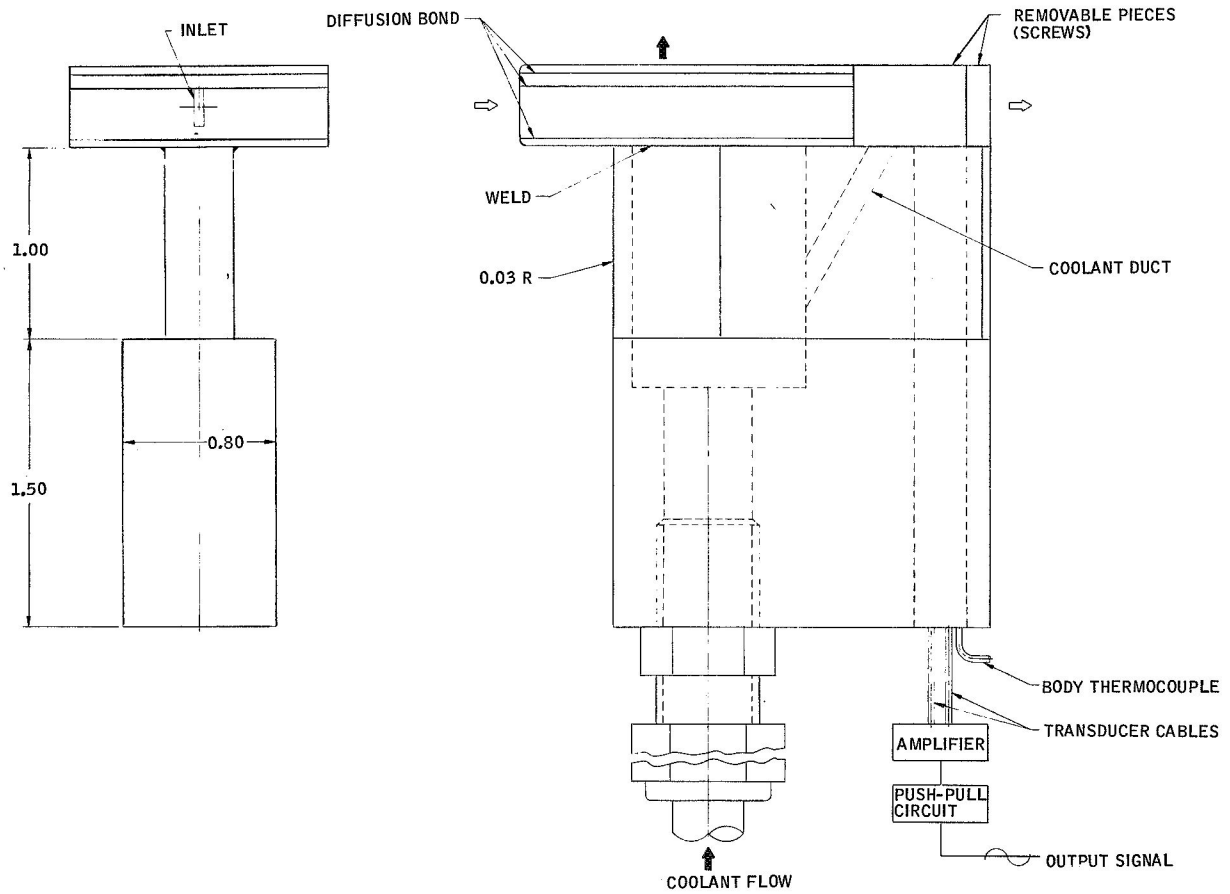
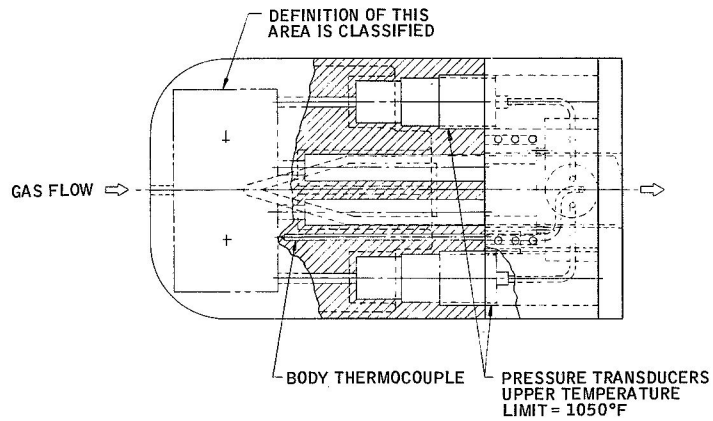


Figure 9. Fluidic Temperature Probe Schematic

The upper section of the pylon which is exposed to the free-stream is formed to a slightly blunted wedge to reduce aerodynamic drag.

Two small pressure transducers are mounted within the oscillator assembly (see Figure 9). The transducers provide a voltage output proportional to the applied oscillating pressure wave. The transducer signals (180 degrees out of phase) are amplified and combined in a push-pull circuit (see PROBE SYSTEM section of this report). The frequency signal may be used with the frequency-to-dc-voltage converters supplied with the sensors.

Air, continually being passed through the fluidic temperature sensor, enters through the small orifice shown on Figure 9. The air is exhausted into the low-pressure base region of the oscillator assembly.

Heat is transferred from the hot air to the sensor body at a rate which requires cooling of the body. Nitrogen gas coolant is ducted into the bottom of the pylon, passed up the leading edge of the pylon, through the oscillator assembly, and dumped overboard out the top of the oscillator assembly (see Figure 9). The nitrogen coolant never interfaces or mixes with the sampled free-stream air. The amount of sensor cooling necessary during flight conditions is discussed in the PROBE SYSTEM section of this report.

The air temperature inside the oscillator is also decreased as the body is cooled. Because cooler gas will oscillate at a lower frequency, an error in the frequency is introduced as the result of cooling. This error is a function of the body temperature and can therefore be corrected for through the measurement of body temperature. This is accomplished with a small chromel-alumel thermocouple placed at the rear of the oscillator cavity wall as shown in Figure 9.

The readout consists, then, of the body temperature and oscillation frequency. In addition, a total inlet pressure must be known to define inlet temperature from the calibration data included in a later section of this report. This requires that a pitot probe be placed alongside the fluidic temperature sensor during the X-15 flight.

The time response of the cooled fluidic temperature sensor is dependent on the purging time of the fluid within the sensor cavity. The purge time is of the order of 10 milliseconds. The exact time depends on the velocity of the gas through the oscillator.

The time for the sensor body to respond to a step change in inlet temperature for the cooled sensor is of no concern because the body temperature is read out continually. For the case of a noncooled sensor where body temperature is not measured, a second time-response term must be considered which is largely a function of sensor mass and the gas flow rate through the sensor.

SENSOR DESIGN

The fluidic temperature sensor assembly and detailed drawings are listed below.

<u>Drawing Title</u>	<u>Honeywell Drawing Number</u>
Bottom Plate	SK 53899
End Plate	SK 53900
Top Plate	SK 53901
Block	SK 53903
Schematic	SK 53905
Layout Probe	SK 53906

Before final hardware was fabricated, a prototype probe was built and tested. A description of the tests is included in a later section, TEMPERATURE TESTS AND CALIBRATION. Independent studies were conducted to provide the basis for the prototype design. These studies were:

- Probe Size Determination
- Rounded Splitter
- Sensor Flow
- Preliminary Temperature Tests

Probe Size Determination

The size of the fluidic temperature probe (see Figure 9) was governed by three factors:

- Oscillator size -- An oscillator cavity size was selected to permit mounting the probe on the X-15 aircraft. The probe is light (about 1 pound without mounting fixture) and small enough to not create a significant amount of aerodynamic drag. A drag coefficient versus Mach number curve for the oscillator assembly alone is shown in Figure 10. Under maximum dynamic pressure conditions, this body will cause a drag of about 10 pounds.

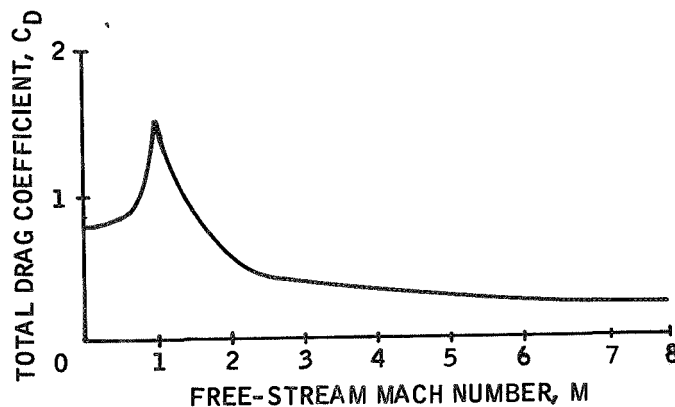


Figure 10. Drag Coefficient versus Mach Number

The oscillator was chosen large enough to generate a sufficiently strong pressure signal to be detected by the KISTLER pressure transducer even at the lower inlet pressures.

The oscillator and its associated coolant ducts, signal transmission line and orifices are of a size to permit fabrication on standard machines.

The oscillator is a desirable size because it operates at frequencies which can be tolerated with no discomfort when not wearing ear protectors during laboratory checks.

- Transducer size -- The pressure transducer (KISTLER Model 601R) was selected because of its miniature size, desired frequency response, and its operating pressure range and upper temperature limit (1500°R).
- Transducer location -- It was decided to mount the KISTLER pressure transducer nearly directly behind the oscillator to minimize signal attenuation and eliminate signal distortion and harmonics which are sometimes present when the signal transmission line must deviate from a straight-line path.

Rounded Splitter

A heat transfer study was conducted to determine minimum internal dimensions of the cooled sensor. Special importance was given to the cooling chamber wall thicknesses and the splitter radius. A sharp splitter could not be used because it would burn away, and the sensor performance would change.

Figure 11 shows the results of a digital computer study of the temperature distribution throughout a splitter configuration. This distribution is created by the offsetting effects of the hot inlet air and the nitrogen coolant gas. The air is shown impacting, then flowing around the splitter. Nitrogen coolant is forced up through the 0.009-inch diameter hole on the centerline and along the back edges of the splitter.

The lines drawn on the splitter are lines of constant $(T_b - T_{Ni})/(T_i - T_{Ni})$ for inlet temperatures in the 4000-5000°R range. Other gas parameters are indicated on the drawing. Many combinations of parameters and splitter configurations were run on the computer. The configuration of Figure 11 was chosen for the final design because its temperature distribution is such that the splitter would never melt down even under the most extreme inlet conditions.

Because a fairly sharp splitter had been used in previous fluidic temperature sensor designs, the effects of the rounded splitter on sensor performance were investigated in the laboratory. An experimental model (number 1) was fabricated. Internal geometry dimensions are classified "Confidential" with a "need to know" obtainable from the Aero Propulsion Laboratory at Wright-Patterson Air Force Base and are not given here so that this work may remain unclassified.

The model was tested to determine signal quality and performance at low inlet pressures. The results of the investigation showed that the rounded splitter sensor performed as well as a sharp splitter configuration.

Sensor Flow

This method of temperature measurement, involving an oscillation of the internal fluid, requires that a fluid jet be provided within the sensor. This, therefore, necessitates a pressure differential across the sensor. The sensor is designed such that a choked-flow condition exists at the sensor exit orifice. Fluids in motion (as in the case of a hypersonic wind tunnel or

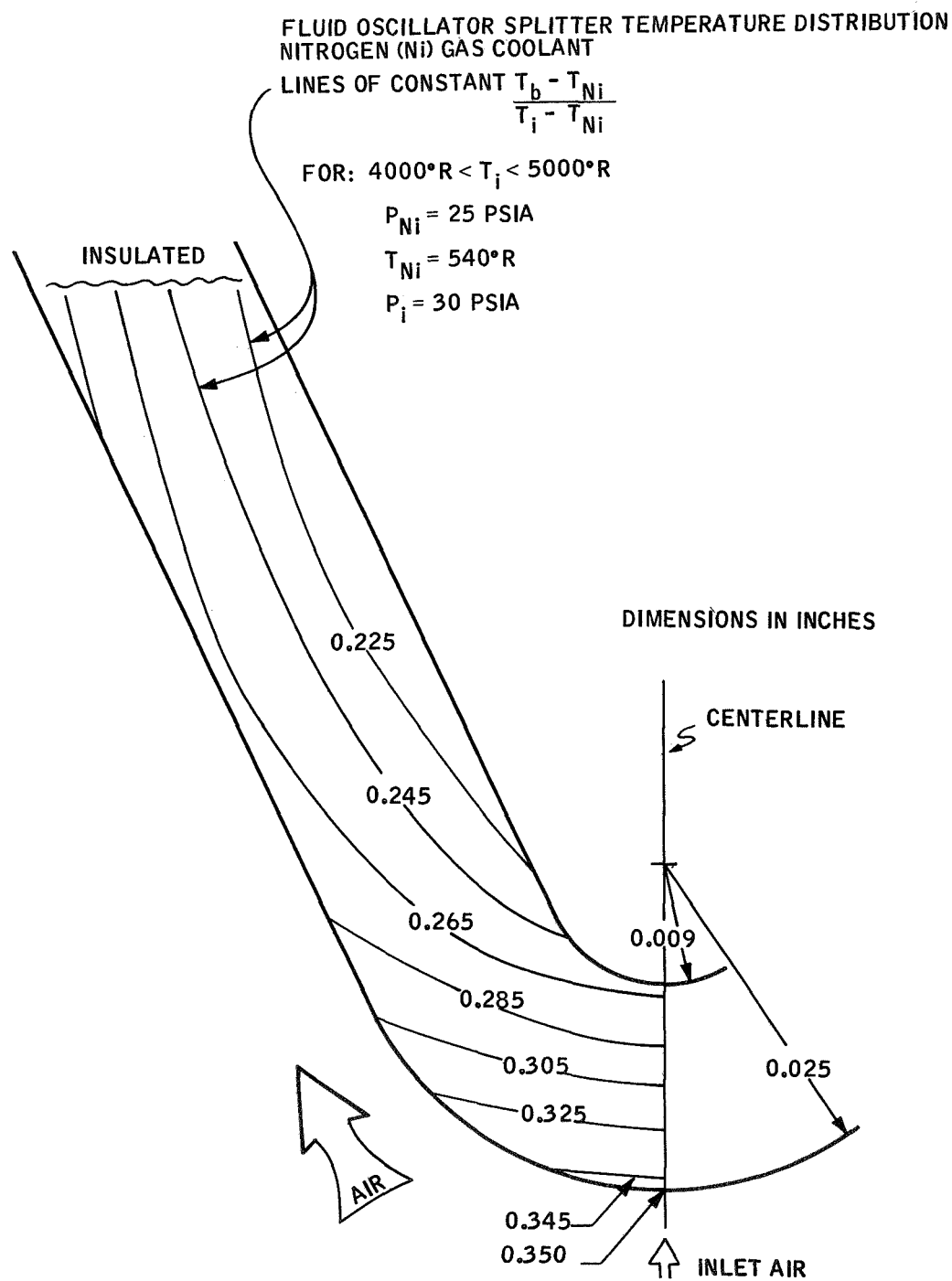


Figure 11. Fluid Oscillator Splitter Temperature Distribution

hypersonic aircraft) provide an adequate pressure drop for the sensor by exhausting into the base region of the sensor where a low static pressure exists. As shown in Figure 12, a pressure ratio across a typical sensor configuration necessary for choked flow occurs at free-stream Mach numbers of about 1.5 and above.

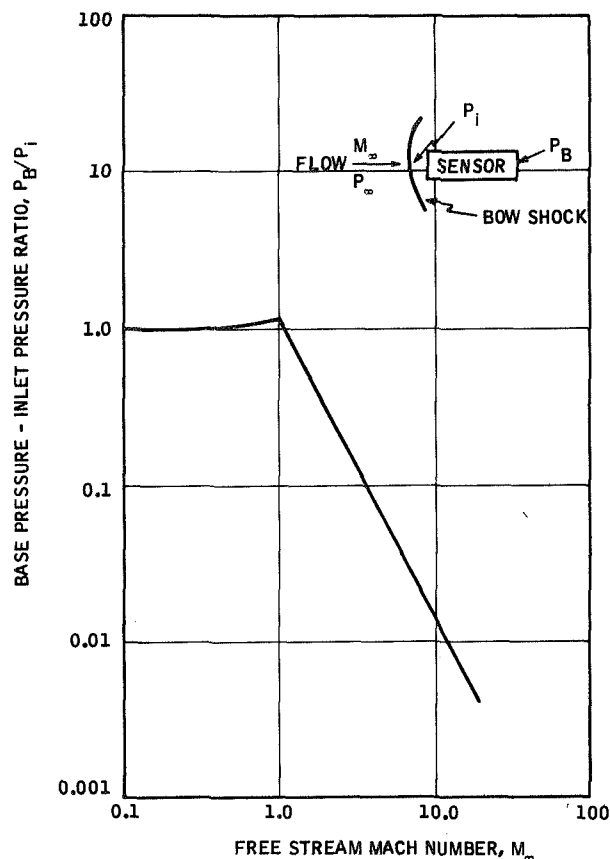


Figure 12. Base Pressure-Inlet Pressure Ratio versus Free-Stream Mach Number

The ratio P_B/P_i presented as a function of M_∞ in Figure 12 was determined from base pressure coefficients for blunted cones from Reference 2 with the aid of Reference 1. The base pressure coefficient is defined:

$$C_{p_B} \equiv \frac{P_B - P_\infty}{\frac{\gamma}{2} P_\infty M_\infty^2}$$

This mode of operation (exhausting into the base region of the sensor) was utilized for one of the high-temperature probes developed for NASA-Ames hypersonic wind tunnels under Contract NAS7-412. This work is reported in Reference 3. It was this particular probe which later flew on the X-15 aircraft (see TESTS ON THE X-15 HYPERSONIC AIRCRAFT section of this report).

The manner in which the flow is ducted from the sensor cavity to the base region is an important consideration from the design and fabrication standpoint. A much simpler design results if the flow leaves at the rear of the cavity and makes no turns in reaching the base region. This point was realized in earlier probe development, Reference 3. At that time a 360-degree swirl configuration was conceived which satisfied the "in-line" flow design. A swirl model (model number 2) was built on Contract NAS4-1211. Preliminary testing showed that this model configuration had a good quality signal and oscillated on very low pressure differentials.

A model (number 3) of a conventional geometry with exit orifices located near the rear of the cavity was also investigated. Feasibility tests showed that this model configuration produced a fine signal and oscillated well at the low inlet pressures (down to 0.5 psia). Because more basic knowledge existed on the conventional geometry, it was selected for the final design over the swirl configuration.

The size of the exit orifices dictates the oscillation frequency dependence on inlet pressure. This is shown by the set of curves of Figure 13 -- data taken at a constant temperature of 512°R (52°F) on model number 3. As seen from the curve for the 0.076-inch diameter exit orifice size, the frequency is nearly independent of inlet pressure from 35 psia down to about 2 psia. At about 0.5 psia the inlet pressure (and therefore cavity pressure) is reduced to a point where the transducer sensitivity is not sufficient to detect the signal. The sensor, however, may continue to oscillate. The frequency-pressure curves can be extended to lower pressures with the aid of a more sensitive detector and more noise-free amplification. Eventually, as inlet

INLET TEMPERATURE CONSTANT AT 512°R (52°F)

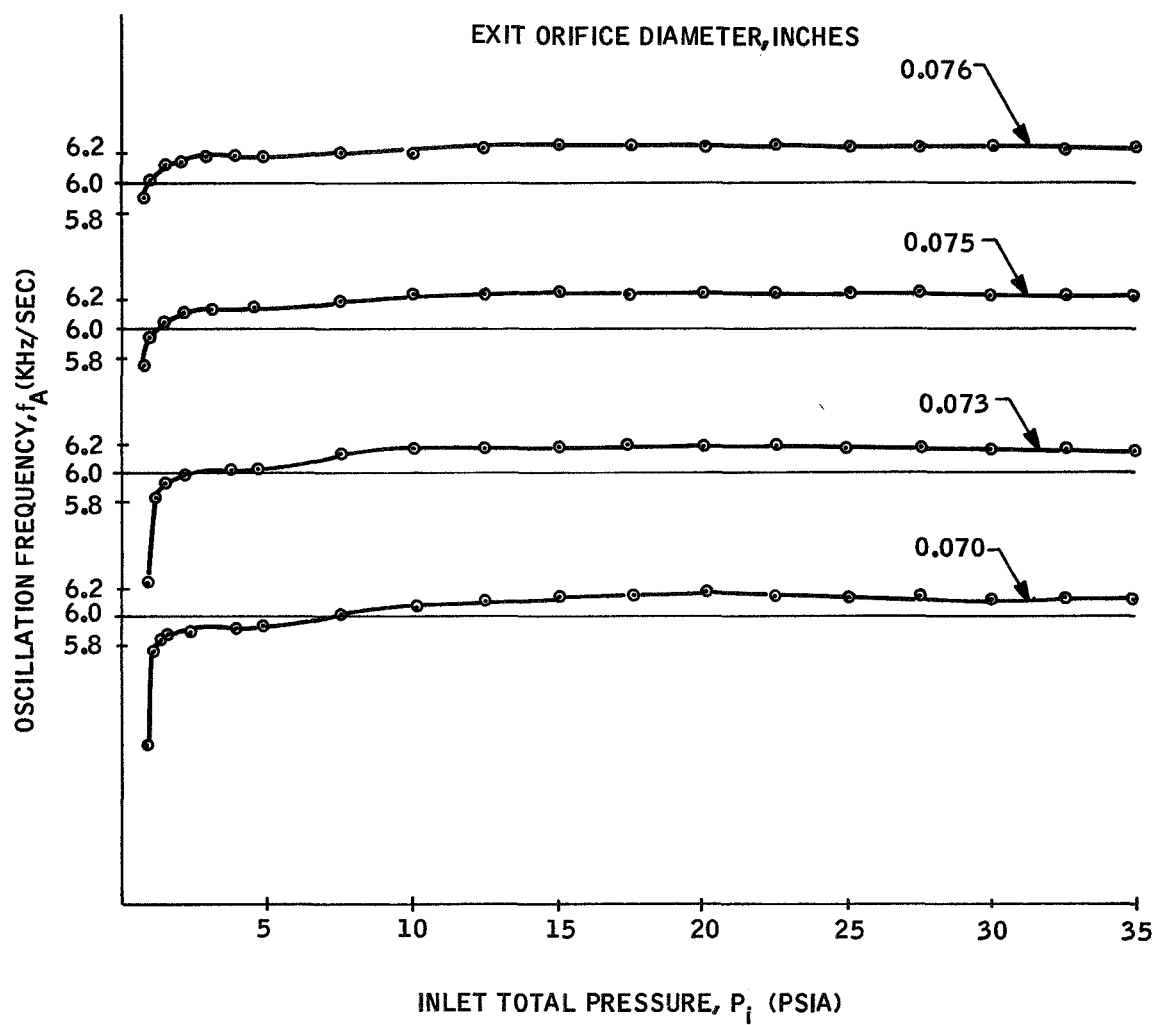


Figure 13. Oscillation Frequency versus Inlet Total Pressure In Air

pressure decreases, the low-density flow doesn't provide enough momentum in the fluid jet to maintain an oscillation.

During the frequency dependence tests the air supplied to the experimental sensor and the sensor body temperature were held constant at 512°R (52°F). This was done by placing the sensor within a temperature controlled environmental chamber shown in Figure 14. The cylindrical shaped styrofoam container held two coiled aluminum tubes which carried air to the sensor and the chamber, respectively. The container was filled with ice and water to regulate the temperature of the air.

Sensor flow and, therefore, sensor performance is also affected by the inlet orifice size. A higher inlet orifice is desirable because it minimizes the cooling effect of the top and bottom cover plates on the cavity gas. (Keep in mind that the sensor cavity flow is two-dimensional.) The ratio of the thickness of the temperature boundary layer on a cover plate to the cavity fluid height should be kept as small as possible without making the overall oscillator height too great for an aircraft probe application.

Preliminary Temperature Tests

A cooled experimental model (number 4) shown in Figure 15 was fabricated and tested at inlet temperatures ranging from room temperature to 2160°R. Model number 4 was a diffusion bonded (see FABRICATION section for details on diffusion bonding) assembly. The inlet gas port and coolant ports are shown in Figure 15.

The model was mounted on a temperature box for the tests. The box contained an electrically heated coil of stainless steel tubing. Air was supplied to one end of the coil, and the sensor inlet port was connected to the coil outlet.

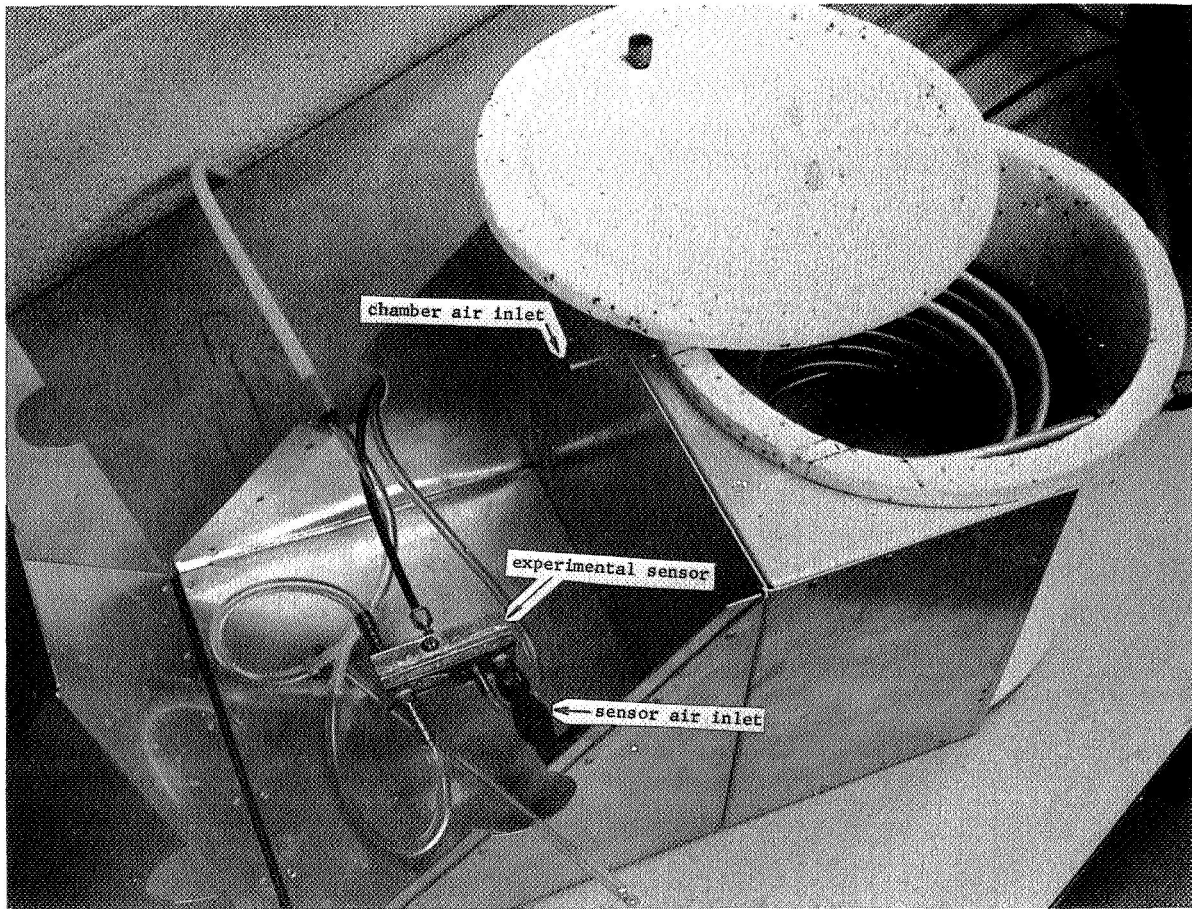


Figure 14. Temperature Controlled Test Chamber

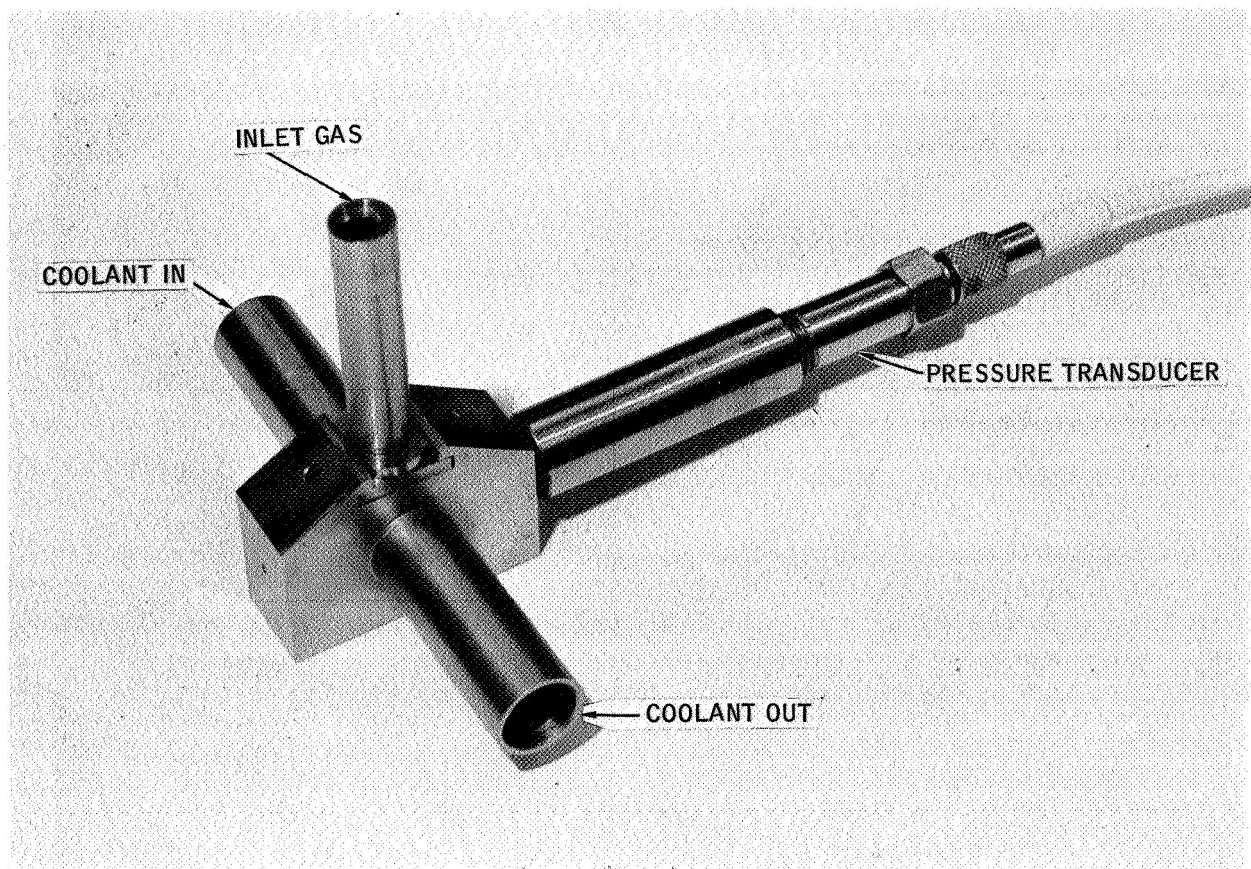


Figure 15. Experimental Cooled Sensor, Model Number Four

Temperature was measured at four places with 0.010-inch-diameter chromel alumel thermocouples. One thermocouple was placed near the inlet, one in the sensor cavity, and two in the body -- just behind the splitter and in the side.

Inlet pressure and coolant flow rate were varied to obtain a wide range of test conditions. The body was cooled to any desired temperature by increasing the coolant mass flow. The signal was read out with the pressure transducer shown in Figure 15.

The experiment proved two points. First, the diffusion bonded assembly can withstand the high thermal gradients created by the hot working gas and cooling gas. There was no evidence of the sensor leaking or coming apart. Second, the experiment proved that it is possible to cool the sensor body to a temperature well below the temperature of the working gas. For an inlet temperature of about 2050°R, it was possible to cool the body to as low as 800°R.

MATERIAL SELECTION

The environmental conditions to which the temperature sensor is subjected dictated the careful consideration given to the material chosen for use in the construction of the probes. Of the important material characteristics, the primary limiting factor is the ability to withstand high-velocity streams of oxidizing gas (air) at high temperature without major oxidation and erosion.

Table 1 shows several materials considered for the cooled sensor. Each candidate material was evaluated from its melt temperature, scaling temperature, coefficient of expansion, machinability and strength at temperature. The information of Table 1 was largely taken from References 4 and 5.

Table 1. Material Characteristics

Material	Temperature Melt Range (°R)	Temperature Scale (°R)	Coefficient of Thermal Expansion 32-1200°R (in/in/°R x 10 ⁻⁶)	Machinability Index	Tensile Strength at 1300°R (psi)
S. S. 304	3000/3100	2100	10.4	55	37,500
S. S. 309	3000/3100	2450	10.0	50	45,000
S. S. 416	3150/3250	1700	6.5	80	13,500
S. S. 431	3050/3150	2050	7.5	--	14,000
S. S. 446	3050/3150	2450	6.4	40	17,000
Hasteloy X	2800	2650	8.3	Very Low	---
Inc. 702	3050	2650	8.5	15	---

Stainless steel 446 has the best overall characteristics for the cooled sensor application. It was selected for the probe material for the following reasons:

- It is machinable.
- It has a high scaling temperature (2450°R), and a high melting point range (3050-3150°R).
- It has a low coefficient of thermal expansion. This is desirable because of the high thermal gradients which exist within a cooled sensor.
- It can be welded.
- It is capable of being diffusion bonded. The bond parameters, 2350°R at 200 psi at three hours results in a bond which has only about 0.5 percent deformation and a shear strength of about 90 percent of the pure material. Shear strength is important because of the high thermal gradients which exist within a cooled sensor.

- It is magnetic and can, therefore, be held down easily during surface grinding -- a necessary step before diffusion bonding.

FABRICATION

For satisfactory operation, the temperature sensor must be an air-tight assembly and be capable of withstanding a large number of heat cycles to high temperatures without warping or leaking. These requirements imposed stringent fabrication techniques on sensor design.

The diffusion bond means of joining the sensor components was selected. The diffusion bond process proved to be very acceptable in fabricating the NASA-Ames hypersonic wind tunnel fluidic temperature sensors, Reference 3. The process, developed during the Ames program, produces a structurally sound and sealed assembly with very little deformation. Further explanation of the diffusion bonding technique can be found in Reference 3.

Before any experimental cooled sensors were fabricated, it was decided to experimentally determine the bond shear strength at a few stainless steel materials. Samples of S. S. 416, S. S. 431, and S. S. 446 were joined under different diffusion bond conditions. See Table 2. The samples were then sheared at the bond plane using a specially designed fixture, Figures 16 and 17, which held the samples in a tensile testing machine. A sheared sample is shown next to the fixture in Figure 17. The samples were pins of 0.1-inch diameter about 0.4 inch long.

As noted in Table 2, the results showed that the shear strength of the bond to be within 87 percent of the pure material for all combinations of the parameters investigated. The bond strength increased slightly with bond time and also with bond pressure.

Table 2. Diffusion Bond Test Results

Material	Bond Pressure (psi)	Bond Time (hr)	Average Shearing Unit Stress (psi)		Length Deformation (percent)
			Pure Material	Bond	
416	400	3	115,500	101,000	1.0
	400	6	115,500	106,000	2.0
431	400	3	118,000	121,500	8.0
	200	3	118,000	120,500	6.8
446	200	3	82,000	72,500	0.6

Note: All bonding was accomplished at 2350°R.

The length deformation, greater for S. S. 431, showed to be a direct function of bond time and bond pressure. This deformation is simply defined as the shrinkage of the sample due to the load.

Once the final three oscillator assemblies were bonded together, they were welded to the pylons with a tungsten-arc process.

PROBE SYSTEM

A photograph of an assembled and a disassembled probe is presented in Figure 18. The probe is designed for mounting in a fixture which in turn is attached to the aircraft. The probe can be held satisfactorily with set screws against the lower portion of the pylon.

The two exit flow orifices noted on the picture lead to the sensor cavity. In leaving the probe, the gas passes through the center block and exhausts into the base region of the probe through the end plate which is held airtight to the probe with the safety wire screws.

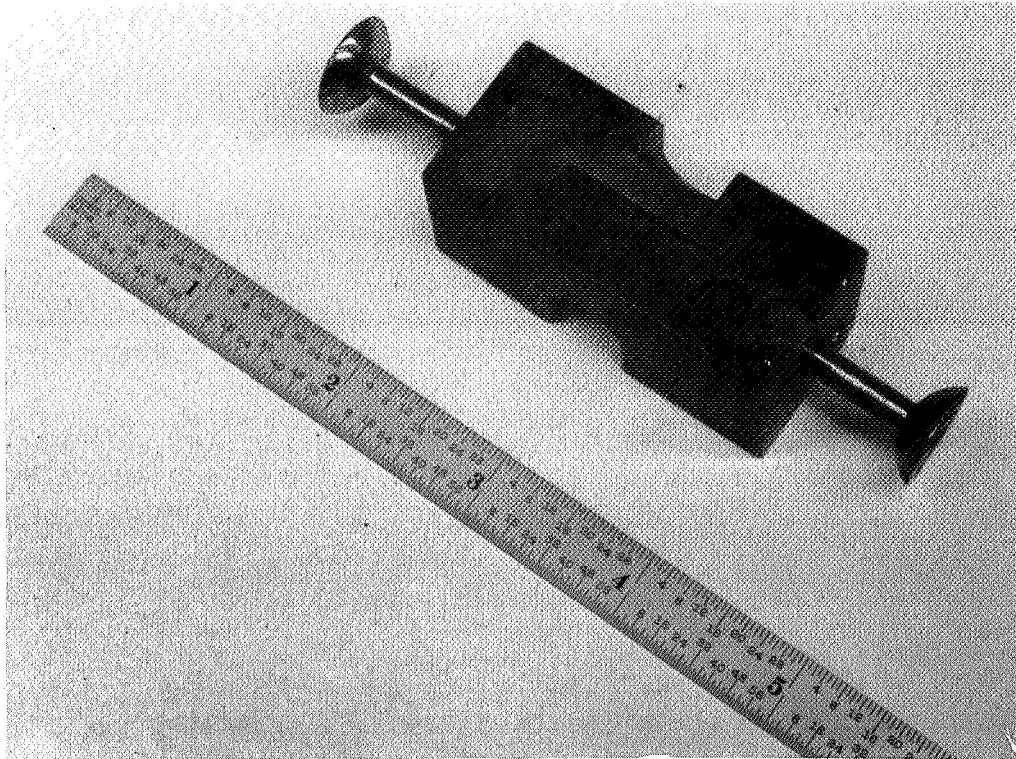


Figure 16. Shear Specimen Fixture, Assembled

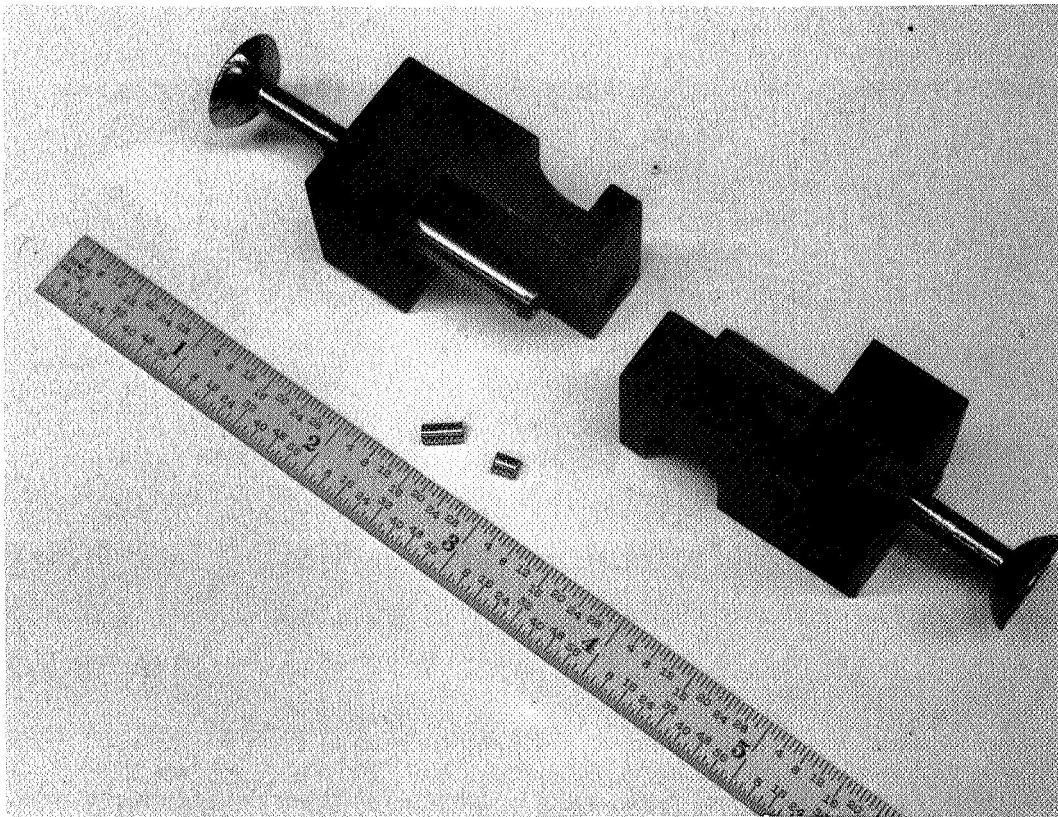


Figure 17. Shear Specimen Fixture, Disassembled

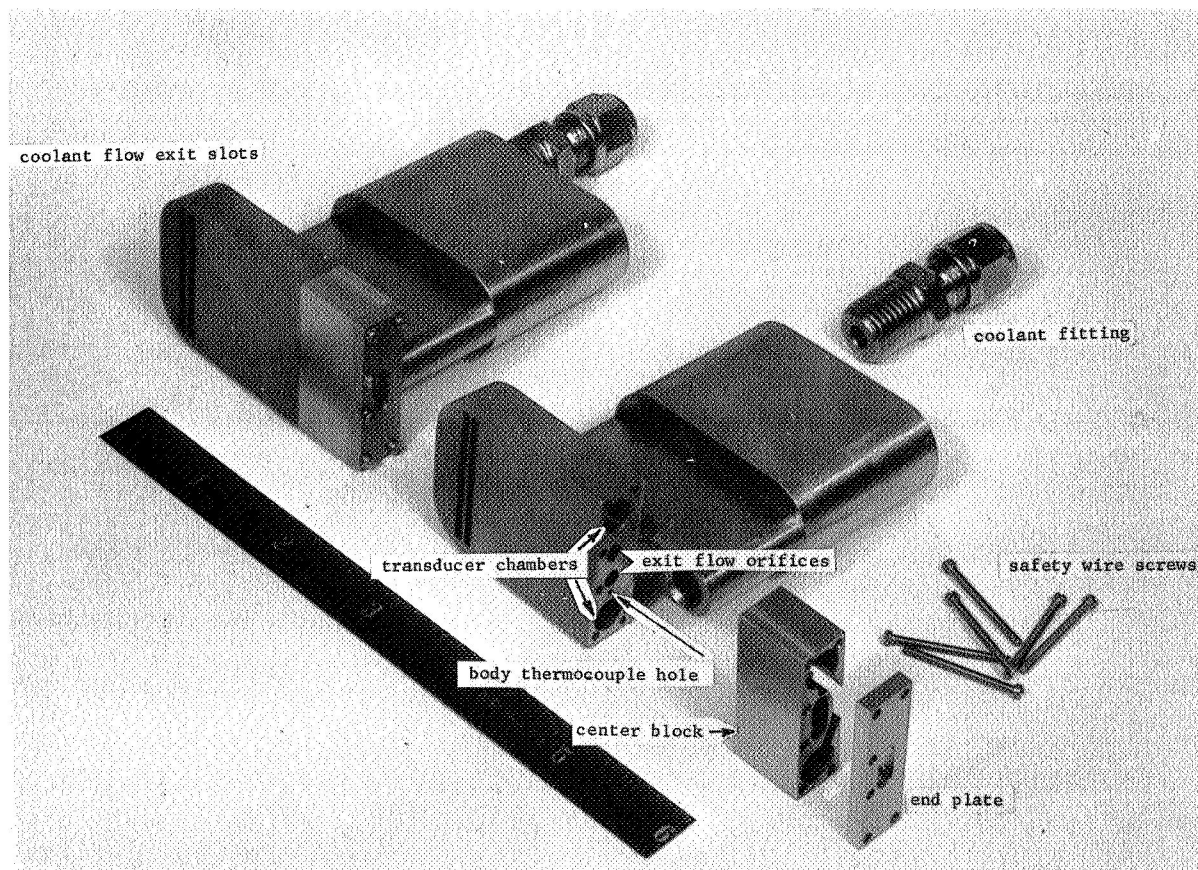


Figure 18. Assembled and Disassembled Probe

The sensor must be disassembled to install the pressure transducers. The transducer cables are inserted up through the rear hole in the pylon, through the center block and into the oscillator assembly. See Figure 18. It is important that the transducers are fully seated in their chambers for optimum signal quality.

The pressure transducer cables were specially fabricated from thermocouple wire (type K with a 0.030 O. D. inconel sheath over M_gO insulation). Like the transducers, the cables can withstand expected temperatures of up to 1500°R. Electrical continuity checks of the cables should be made prior to the flight. Replacement of cables is discussed in the contract Operating Instruction Manual, Honeywell Document 12080-OIM-1.

Coolant System

Heat is transferred from the hot air to the sensor body at a rate which requires cooling of the body. Nitrogen gas coolant is ducted into the bottom of the pylon, passed up the leading edge of the pylon (through a hole fashioned by an EDM process), through the oscillator assembly, and dumped overboard out the exit slots located on the top of the probe (see Figure 18).

A schematic of a simple coolant system is shown in Figure 19. A pressure regulator followed by a choked orifice will establish a constant flow rate from the pressurized nitrogen gas bottle. The regulator can be set prior to the flight.

The amount of sensor cooling necessary during flight conditions depends on the free-stream Mach number, stagnation pressure and aircraft total temperature-time history. Because these flight parameters are approximately known prior to the flight, the maximum required coolant flow rate can be estimated from data taken in the Honeywell laboratory during calibration of the probes.

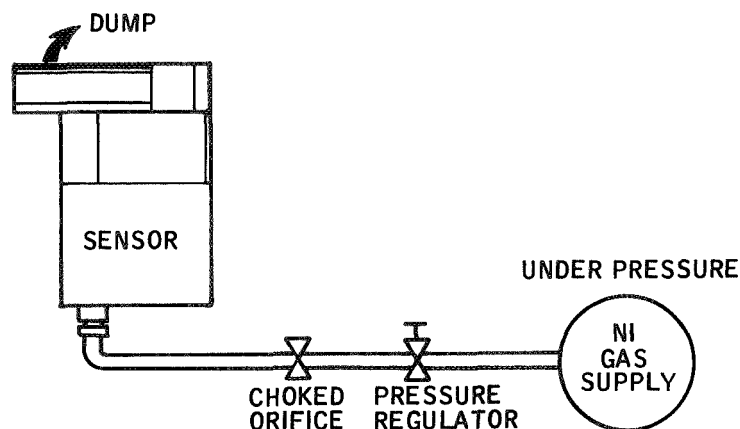


Figure 19. Schematic of Coolant System

This data is presented in Figures 20 through 23. For example, if the maximum expected inlet temperature is 4000°R at about 4.5 psia, and the desired body temperature is 1300°R , the coolant flow rate must be regulated for 2.0 scfm. The required rate would be less if the inlet total pressure was lower.

Readout Electronics

The temperature sensor makes free-stream total temperature measurements on aerospace vehicles and transforms these measurements into electrical signals. The electrical signals monotonically increase with increasing total temperature.

Two KISTLER pressure transducers (see Appendix B for specifications) are used to detect the fluidic oscillator signal. The transducer puts out a voltage which is proportional to the applied alternating pressure. The transducers are arranged to operate in push-pull, with either transducer capable of independent operation should the other fail.

The signal is transmitted from the transducer to the electronic readout circuit via a specially designed cable (described earlier).

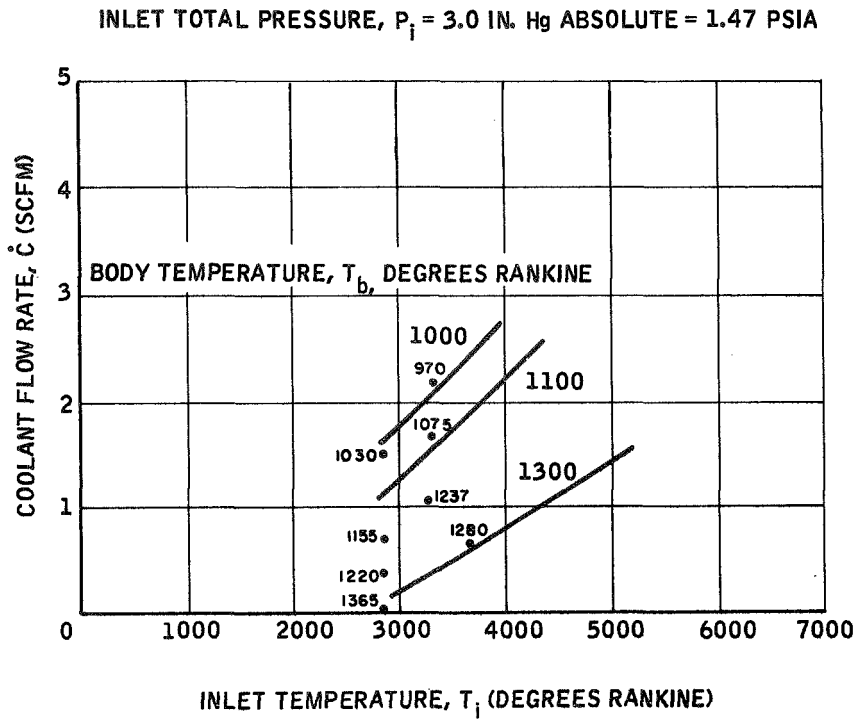


Figure 20. Coolant Flow Rate versus Inlet Temperature,
Inlet Total Pressure = 3.0 in. Hg_{ABS}

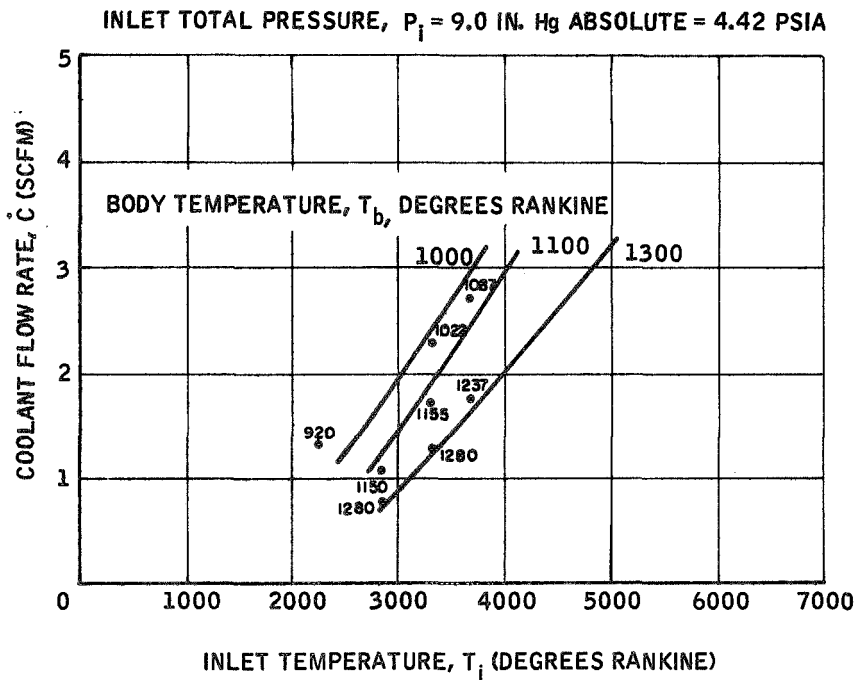


Figure 21. Coolant Flow Rate versus Inlet Temperature,
Inlet Total Pressure = 9.0 in. Hg_{ABS}

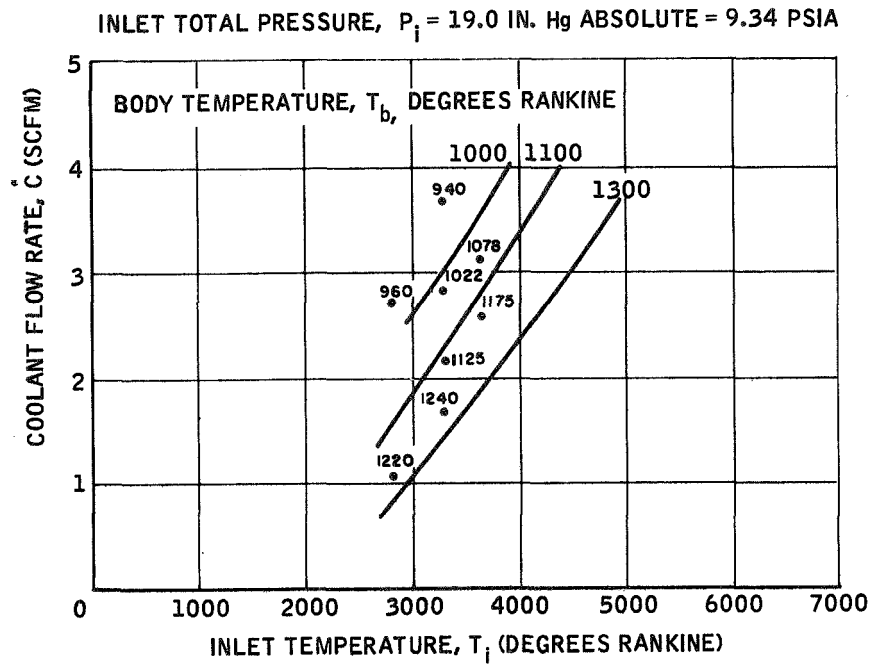


Figure 22. Coolant Flow Rate versus Inlet Temperature,
Inlet Total Pressure = 19.0 in. Hg_{ABS}

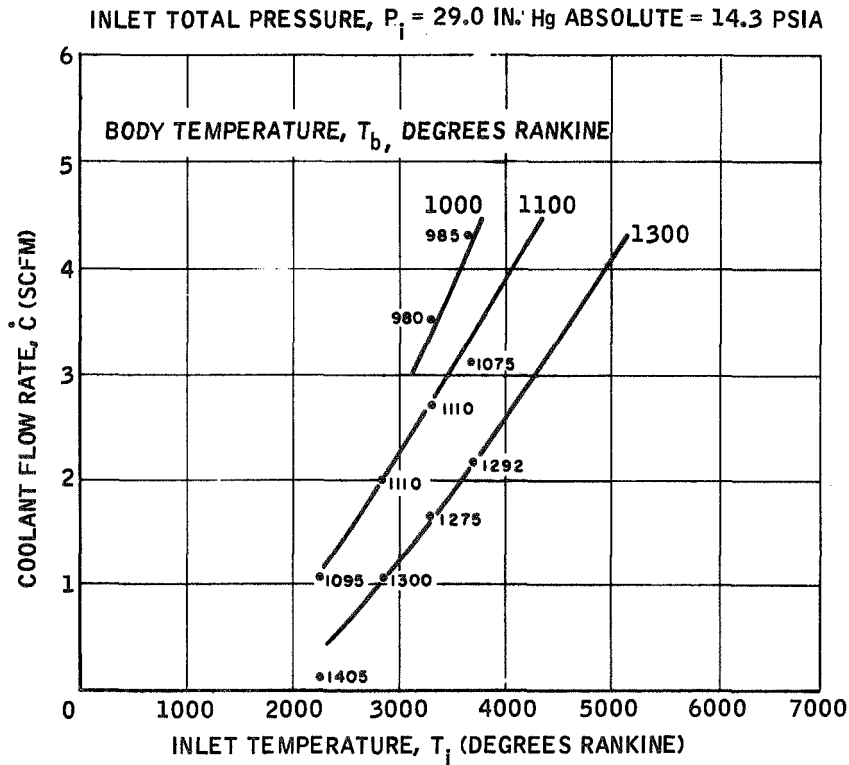


Figure 23. Coolant Flow Rate versus Inlet Temperature,
Inlet Total Pressure = 29.0 in. Hg_{ABS}

The electronic circuit, shown schematically in Figure 24 amplifies and conditions the transducer signals for a frequency-to-dc-voltage converter. Any d-c pressure changes which might be detected by the transducers are cancelled out thus eliminating the d-c effects in the output. Output voltage of the circuit is shown versus the input signal frequency in Figure 25.

A photograph of three electronic packages delivered to NASA is included as Figure 26. The packages were designed and built to withstand the environmental conditions experienced by the X-15 aircraft. Package tests for these conditions are discussed in the ENVIRONMENTAL REQUIREMENTS section of this report. Military specification MIL-E-5400, "Electronic Packaging of Airborne Equipment" was used as a reference in assembling the electronic components. A description and specifications of the components are included in Appendix B. In addition to the listed specifications, the individual components also meet the environmental requirements.

A sketch showing the outside dimensions of the aluminum package is shown in Figure 27. The eight screws which fasten down the cover plate to the plate may be wired for safety. The electronic processing equipment meets the following requirements:

- Input power: 115 vac ± 5 vac, 400 Hz ± 20 Hz
- Output: Full-scale output of 0 to +5 vdc
- Grounding: Separate ground return wires are provided for the power input and for the signal output. The electronics case shall not be used as a common ground.
- Polarity reversal: Inadvertent reversal of input power shall not damage the instrument or cause a change in the performance.
- Shorting: Shorting the output signal shall not damage the instrument or cause a change in the performance.

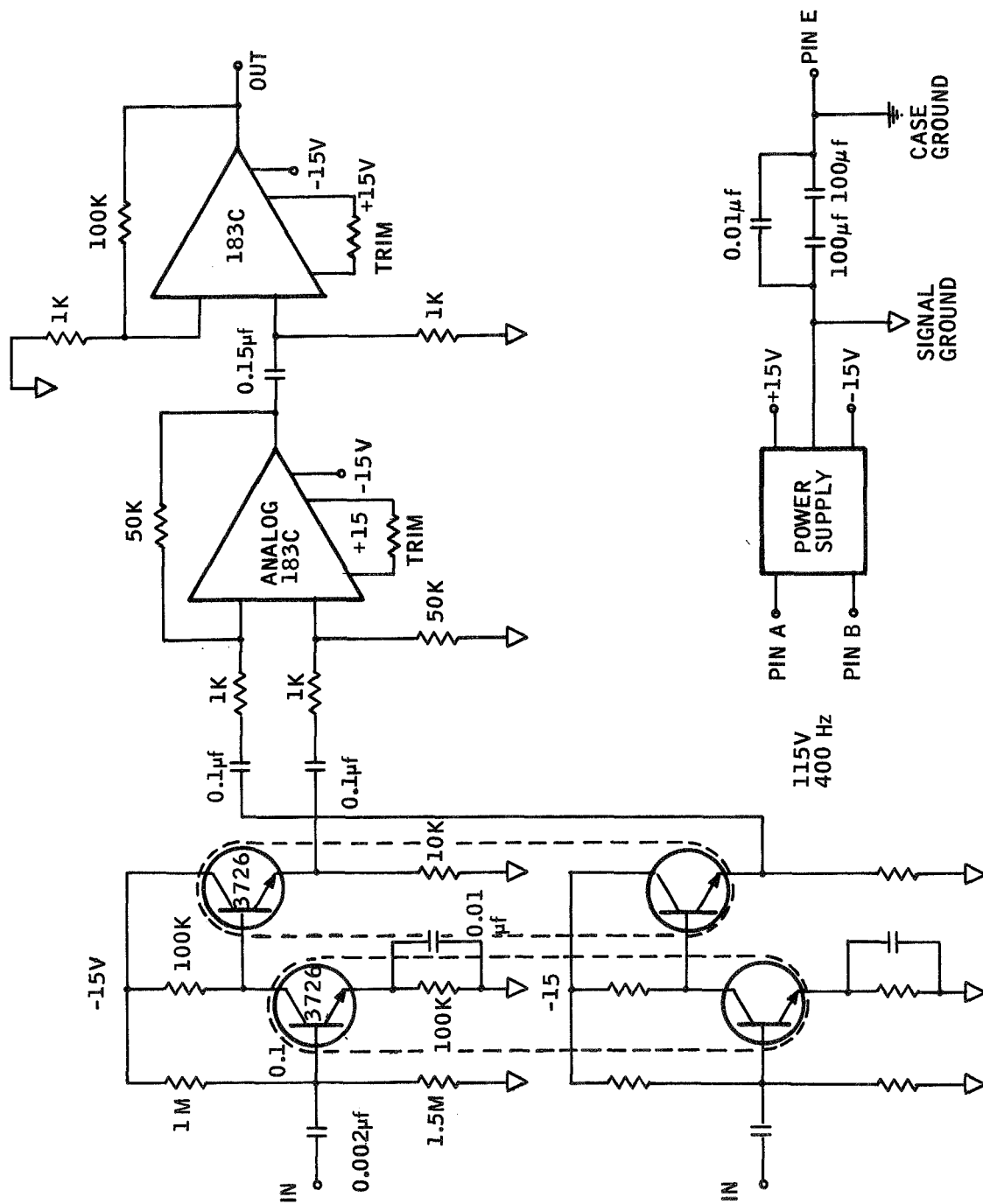


Figure 24. Schematic of the Electronic Readout Circuit

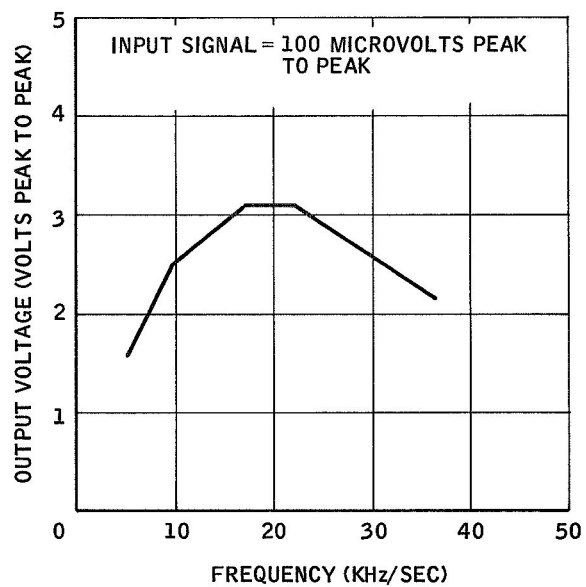


Figure 25. Output Voltage versus Frequency

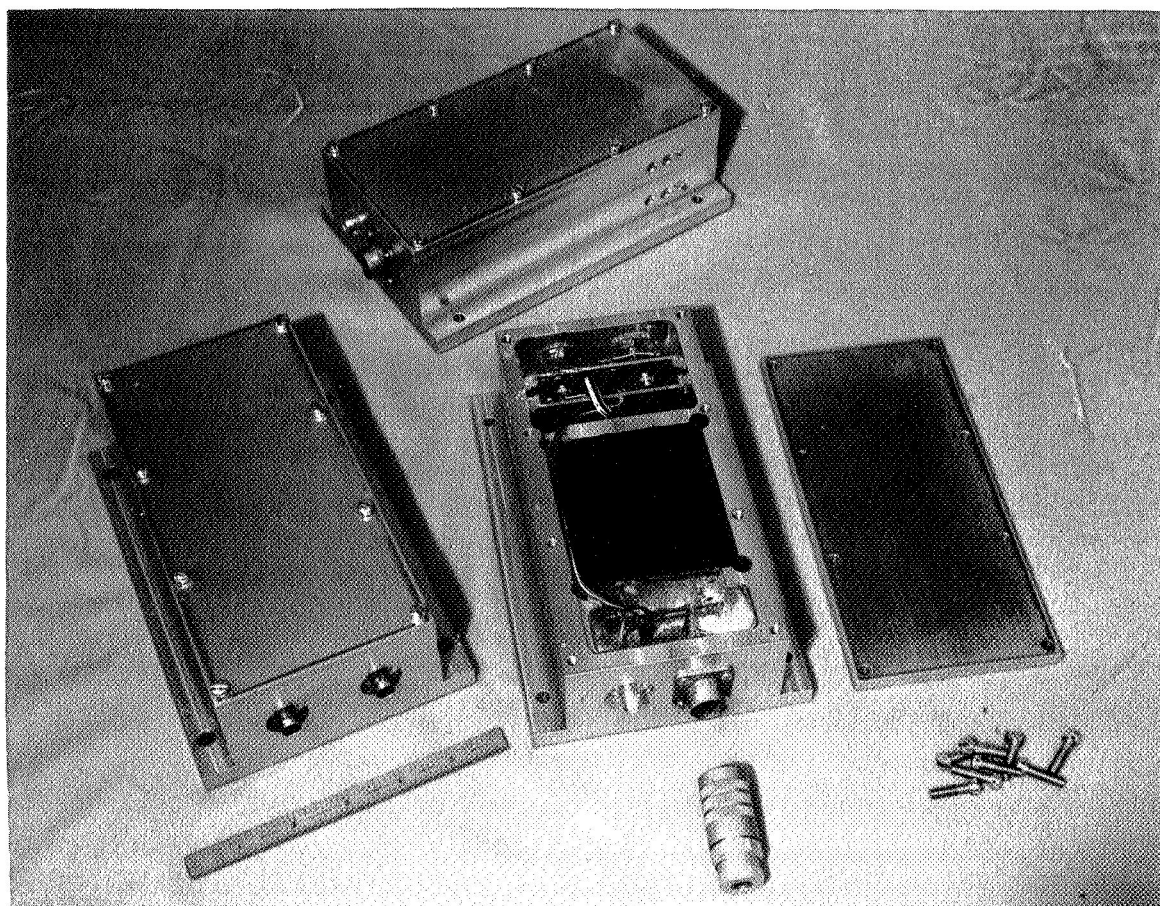


Figure 26. Three Electronic Readout Packages

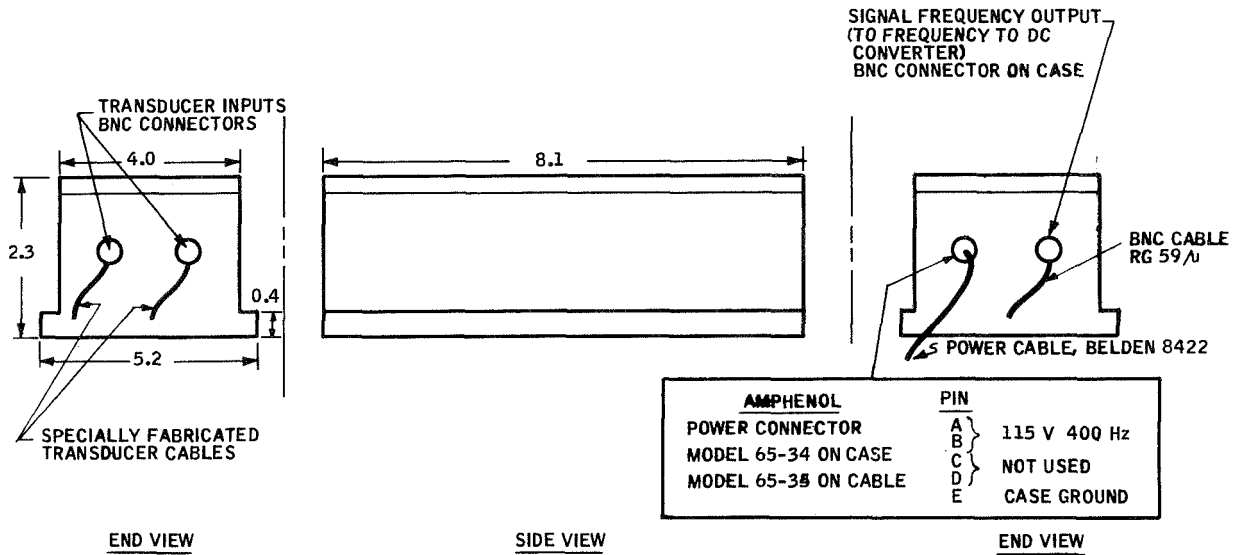


Figure 27. Electronic Package Sketch

TEMPERATURE TESTS AND CALIBRATION

This section includes a description of the temperature test facilities and the calibration data obtained on the delivered probes.

Low-Temperature Tests

Low-temperature data (up to 1660°R) was obtained on the prototype probe with a temperature box which enclosed an electrically heated coil of stainless steel tubing. Nitrogen gas was supplied to one end of the coil, and the probe was mounted at the other end as shown in Figure 28. The gas was heated to desired temperatures as it passes through the coil.

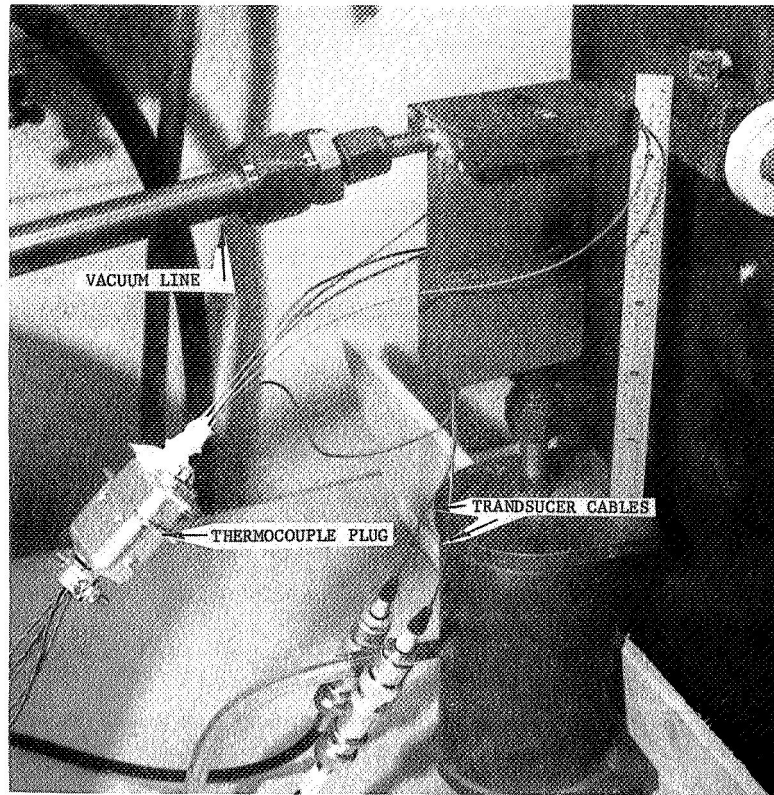


Figure 28. Prototype Fluidic Temperature Probe

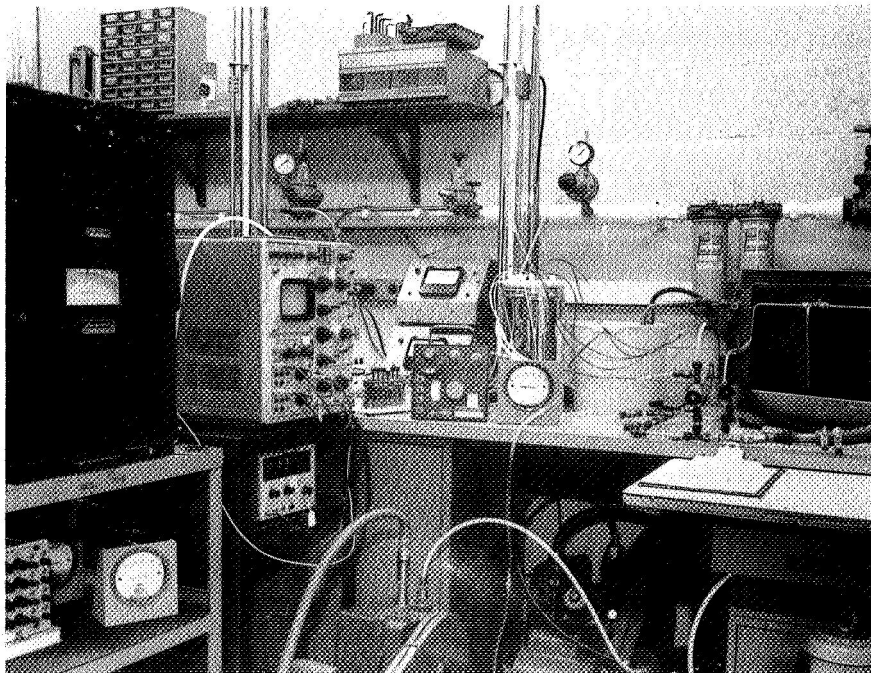


Figure 29. Temperature Box and Test Equipment

The gas pressure within the coil was regulated with a vacuum pump, which pulled gas through the sensor, and a valve in the gas line which fed the coil. The equipment used to monitor the sensor performance during the tests is shown in Figure 29.

The sensor was instrumented with 0.010-inch-diameter chromel-alumel thermocouples which measured the following temperatures:

- Inlet gas
- Cavity gas
- Sensor body
- Pressure transducer

A parametric study was conducted to obtain data on the following variables:

- Inlet temperature (1060°R and 1660°R)
- Inlet pressure (1.5 psia to 24.0 psia)
- Oscillation frequency
- Body temperature which varied with coolant rate (Nitrogen)

The data from the low-temperature tests is presented later along with the high-temperature data and is also tabulated in Appendix A.

High-Temperature Test Facility

All of the high-temperature (2260°R and above) data was obtained in the STOKES resistance furnace located at the Honeywell Corporate Research Center located in Hopkins, Minnesota.

The STOKES furnace, pictured in Figures 30 and 31, consists of a large cylindrical chamber which contains a heating element -- usually carbon

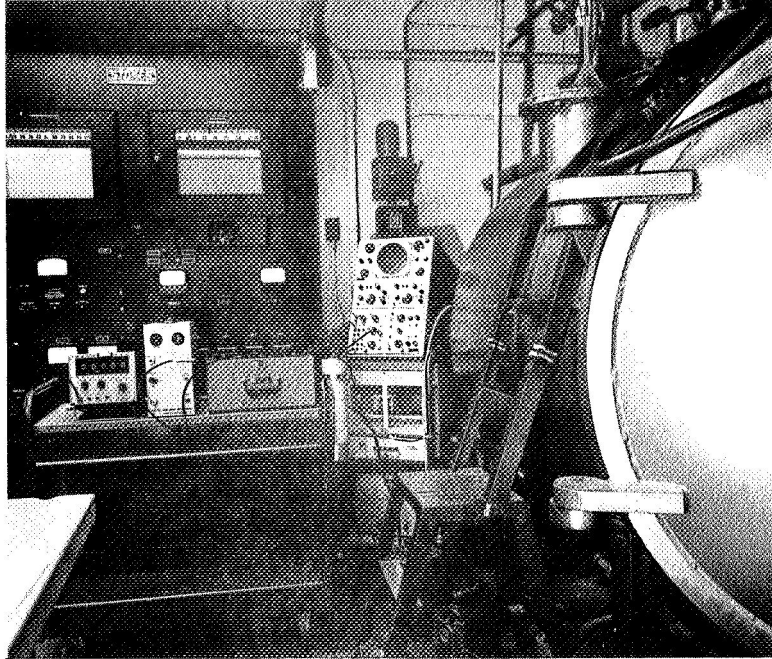


Figure 30. STOKES Resistance Furnace - Outside View

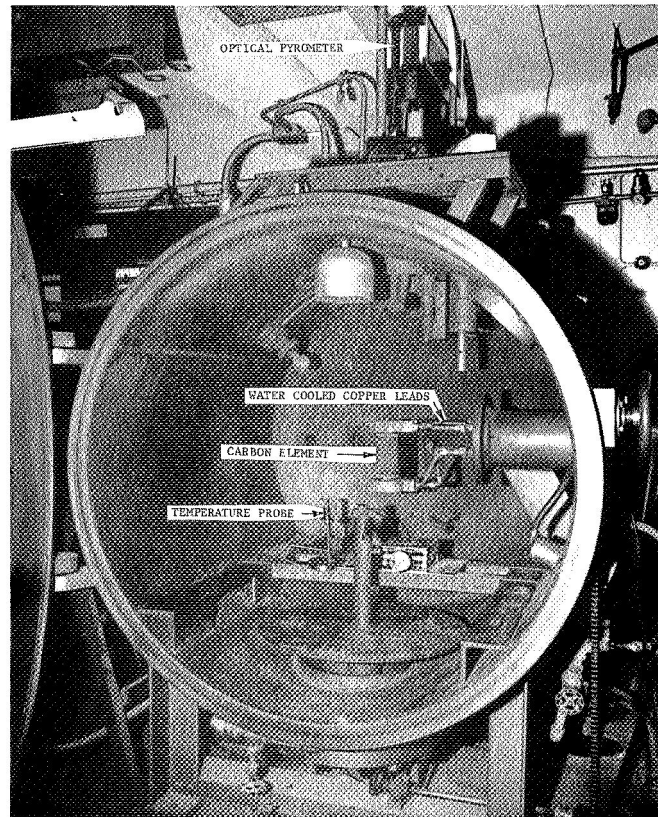


Figure 31. STOKES Resistance Furnace - Inside View

material. The element is supported between two copper electrodes or leads which are connected to a transformer and 50-kw commercial power supply. Electrical power (I^2R) is dissipated within the element.

Because the carbon element will burn in air, the large furnace chamber is evacuated before the power is turned on. The vacuum system which is capable to less than 1 micron consists of a large roughing pump and a diffusion pump. The chamber was backfilled with nitrogen to the desired pressure up to one atmosphere. It is this pressure that is equivalent to sensor inlet total pressure.

A schematic drawing of the high-temperature calibration setup in the STOKES furnace is shown in Figure 32. The inlet portion or snout of the fluidic temperature sensor was inserted into the carbon element as shown in Figure 33. The sensor was held rigid with respect to the element with a fixture. The distance that the probe was inserted into the carbon hot-zone established a temperature profile from the leading edge back along the oscillator assembly.

Gas was pulled through the sensor to make it oscillate. (See SENSOR OPERATION section for a schematic of the sensor showing the hot working gas path.) The gas was heated up as it passed from the large chamber into the carbon hot-zone through about 200 small holes. The same vacuum pump that was used to pull down the furnace chamber was used to drive the oscillator. The gas was cooled before it entered the vacuum pump by coiling the gas line in a water tank.

When the sensor was mounted in the carbon element, it didn't make contact with the carbon, thus preventing heat conduction from the carbon to the sensor. The gap between the sensor and the carbon was sealed with an insulating material to prevent gas from entering through the gap. Two materials have been used satisfactorily to form this seal -- a matted quartz fiber and a refractory fiber felt formed from alumina-silica-chromia fibers having a melting point over 3500°R.

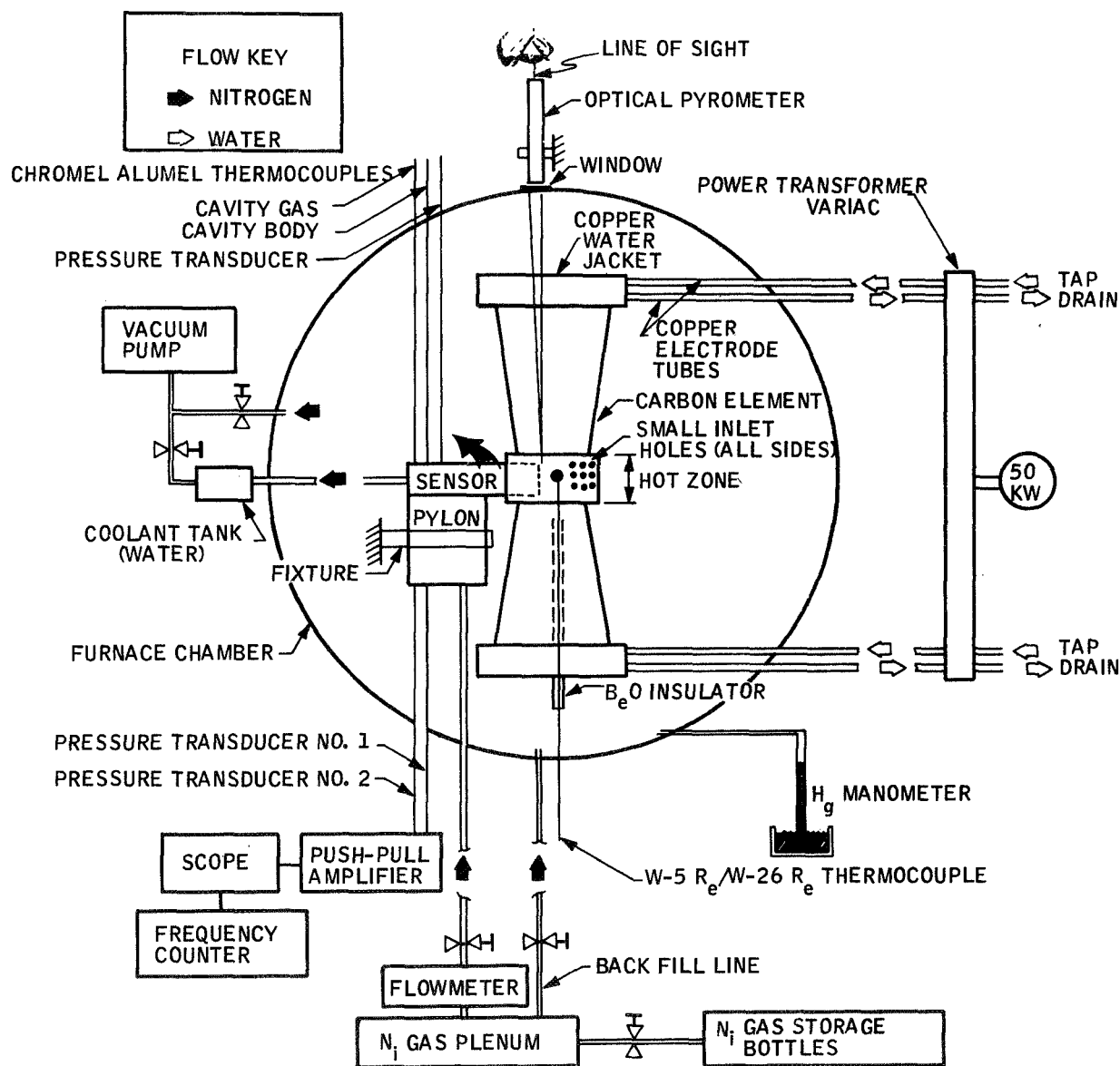


Figure 32. Schematic of High-Temperature Calibration Setup

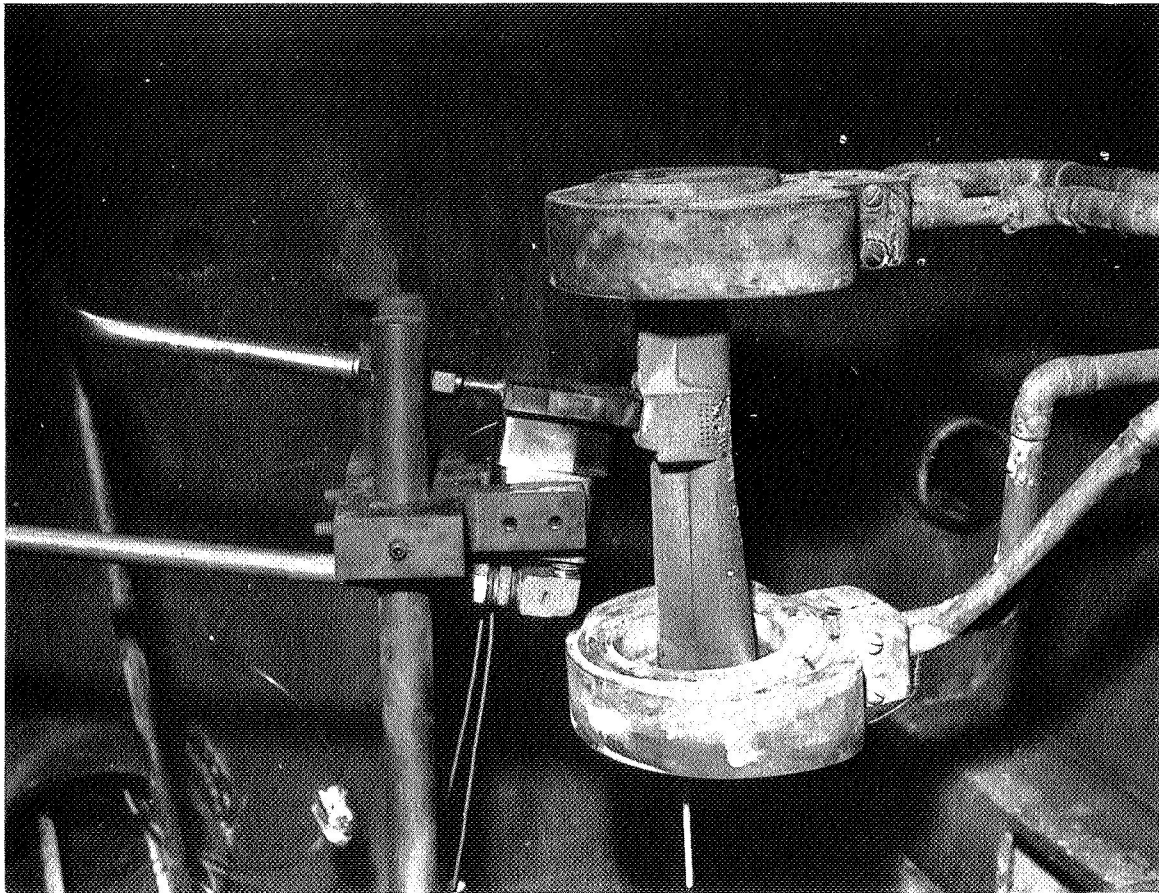


Figure 33. Temperature Probe Ready for Test

The carbon elements used for fluidic temperature sensor tests were easily machined from solid stock. The cross sections of the elements vary from plain cylinders (like the one pictured in Figure 31) to more complicated configurations like that pictured in Figure 33. In designing the element cross sections, a tradeoff existed between structural strength and electrical resistance. A low cross sectional area is desirable because it offers more resistance and, therefore, may be heated to higher temperatures. The cross-sectional areas were kept small to minimize heat conduction from the carbon to the water-cooled copper jackets which held the ends of the element.

All thermocouples and pressure transducer electrical cables were taken outside the furnace chamber through an access plate which was sealed to the chamber wall by an 'O' -ring.

Thermocouple. - The element was fabricated with provisions for holding a thermocouple which was used to measure the hot-zone gas temperature. See Figure 32. Because the thermocouple ball was completely surrounded by hot carbon walls which were very nearly the same temperature as the gas (verified with an optical pyrometer), there were no significant thermocouple radiation errors.

A tungsten -- 5 percent rhenium versus tungsten -- 26 percent rhenium thermocouple was used with success. The millivolt versus temperature curve for this thermocouple is shown in Figure 34. The curve slope is fairly constant over the thermocouple measuring range of 0 to 4500°R. There are indications in the literature that a dinitride is formed with tungsten at a temperature of about 4660°R and that moist nitrogen may attack rhenium above a temperature of about 4000°R. Dry nitrogen was used for all tests.

Another limiting factor in thermocouple temperature measuring capability was the insulator used with the thermocouple. Beryllium oxide insulation loses its insulating properties to a point where the emf indication of the thermocouple is seriously affected at temperatures above 4460°R.

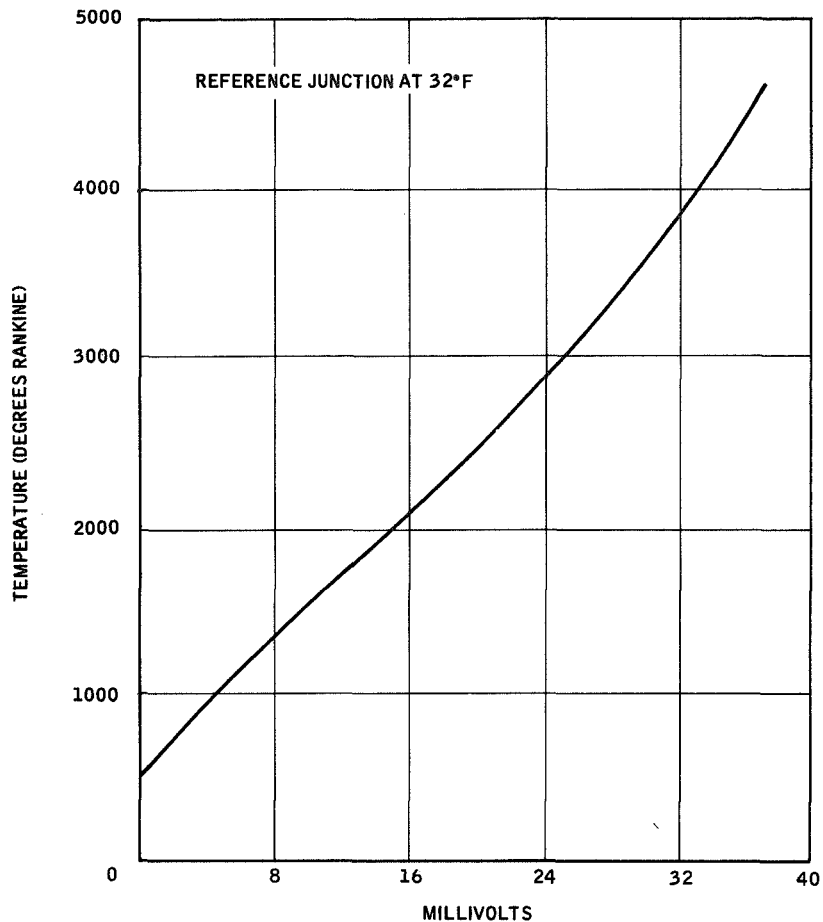


Figure 34. Temperature - Millivolt Equivalent for a Tungsten - 5 Percent Rhenium versus Tungsten - 26 Percent Rhenium Thermocouple

Pyrometer. - Another hole was fashioned in the carbon element for viewing the hot zone with an optical pyrometer. See Figure 32. A piece of glass laid over the top of the hole prevented cold gas from entering the hot zone via this hole. A pyrometer was used to measure the sensor body temperature and the carbon temperature. Because the gas velocity was low inside the hot zone, the carbon was very nearly the same temperature as the gas. This has been proven with many comparisons between the pyrometer and thermocouple measurements. All comparisons have been within 2.0 percent, and the majority within 1.0 percent. The pyrometer readings serve as backup data for the thermocouple. This double reading immediately indicated whether the thermocouple was operating satisfactorily.

All pyrometer measurements were corrected for material emissivity and lens error.

High-Temperature Tests

When testing and calibrating the fluidic temperature probes, it is, of course, desirable to match the operating or flight environmental conditions in the laboratory (see INLET CONDITIONS section for these conditions). Although it is not possible to simulate the complete flow field which would exist around the probe, it was possible to match some inlet gas pressures and temperatures.

It was also possible in the laboratory to establish body temperature profiles (from the leading edge back along the oscillator assembly) which approximate the profiles that would occur during actual flight.

The actual temperature profile on the sensor during flight conditions depends on the free-stream Mach number, stagnation pressure, the aircraft total temperature-time history. Temperature profiles for a similar problem have been determined analytically. This analysis, for the radiation shroud used on the NASA-Ames fluidic temperature sensors, is discussed in Reference 3. Using the information from Reference 3 and X-15 flight performance data, typical temperature profiles can be roughly determined as shown in Figure 35.

During the laboratory tests, similar profiles were established by varying the distance that the probes were inserted into the carbon element hot-zone.

Honeywell tested and evaluated the final sensors to demonstrate that all requirements specified in Contract NAS4-1211 were met. Prior to testing, all sensors were identical in mechanical design, were in operational form and contained all modifications deemed necessary to meet the specified requirements.

Testing was performed in accordance with the Contract Test Plan, Honeywell Document 12080-TP1. The environmental evaluation is described in the ENVIRONMENTAL TEST section of this report. The temperature testing portion of the Test Plan is presented here.

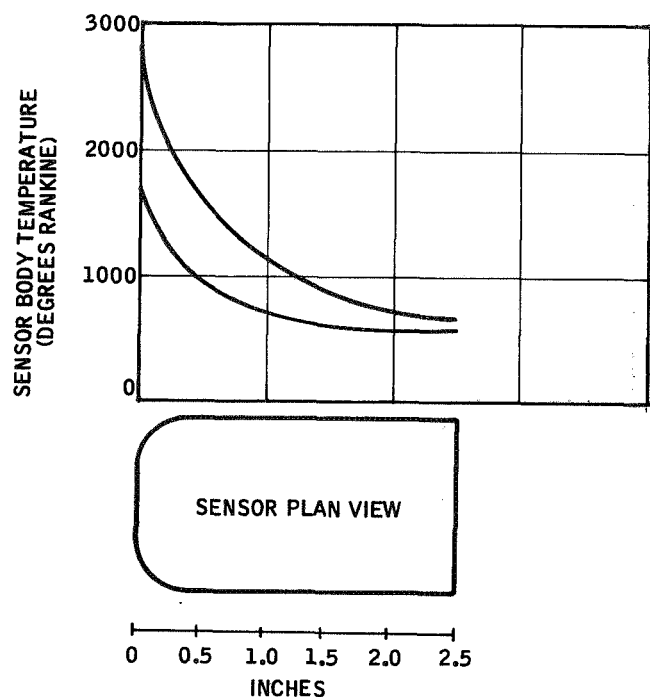


Figure 35. Typical Sensor Body Temperature Profiles

All three probes delivered were tested in the STOKES resistance furnace in a nitrogen atmosphere. One of the probes was tested at room temperature only. All the readings taken for all three probes agreed. One probe was subjected to 105 percent of stated range or 4200°R. Testing consisted of duplicating within ± 2 percent of reading several test points on one of the three (3) probes delivered.

A fourth probe, not delivered (the prototype) was tested through twenty (20) temperature cycles from about 3000°R to 4100°R. The inlet temperature was held constant for 60 seconds at 4100°R for each cycle. The prototype probe was also subjected to 4400°R inlet temperature without damage to the probe.

Calibration data were taken with a tungsten -- 5 percent rhenium versus tungsten -- 26 percent rhenium thermocouple. An optical pyrometer was used to make approximate temperature readings to back up the thermocouple

data. The thermocouple failed during a few of the very high temperature tests. The failure was caused by the melting of the beryllium oxide insulator and subsequent shorting of the thermocouple wires. At the higher inlet temperatures the carbon element sublimed slowly, and carbon built up in the probe inlet orifice. The orifice was checked and cleaned prior to each run.

The calibration data are presented in Figures 36 through 39, each figure representing data at a different inlet total pressure. The calibration data is tabulated in Appendix A.

The calibration data in Figures 36 through 39 have been cross plotted to form calibration curves shown in corresponding Figures 40 through 43. The calibration figures show inlet temperature plotted against oscillation frequency for three body temperature values -- 1000°R, 1100°R and 1300°R.

The temperature probes were tested and calibrated in nitrogen gas. All of the plots presented here are for air. The oscillation frequency data was corrected to air by the following analysis:

The basic equation which describes the fluidic oscillator may be written

$$f = \frac{\sqrt{\gamma R T_c}}{\lambda}$$

The expression for air is

$$f_A = \frac{\sqrt{\gamma_A R_A T_c}}{\lambda}$$

and for nitrogen

$$f_{Ni} = \frac{\sqrt{\gamma_{Ni} R_{Ni} T_c}}{\lambda}$$

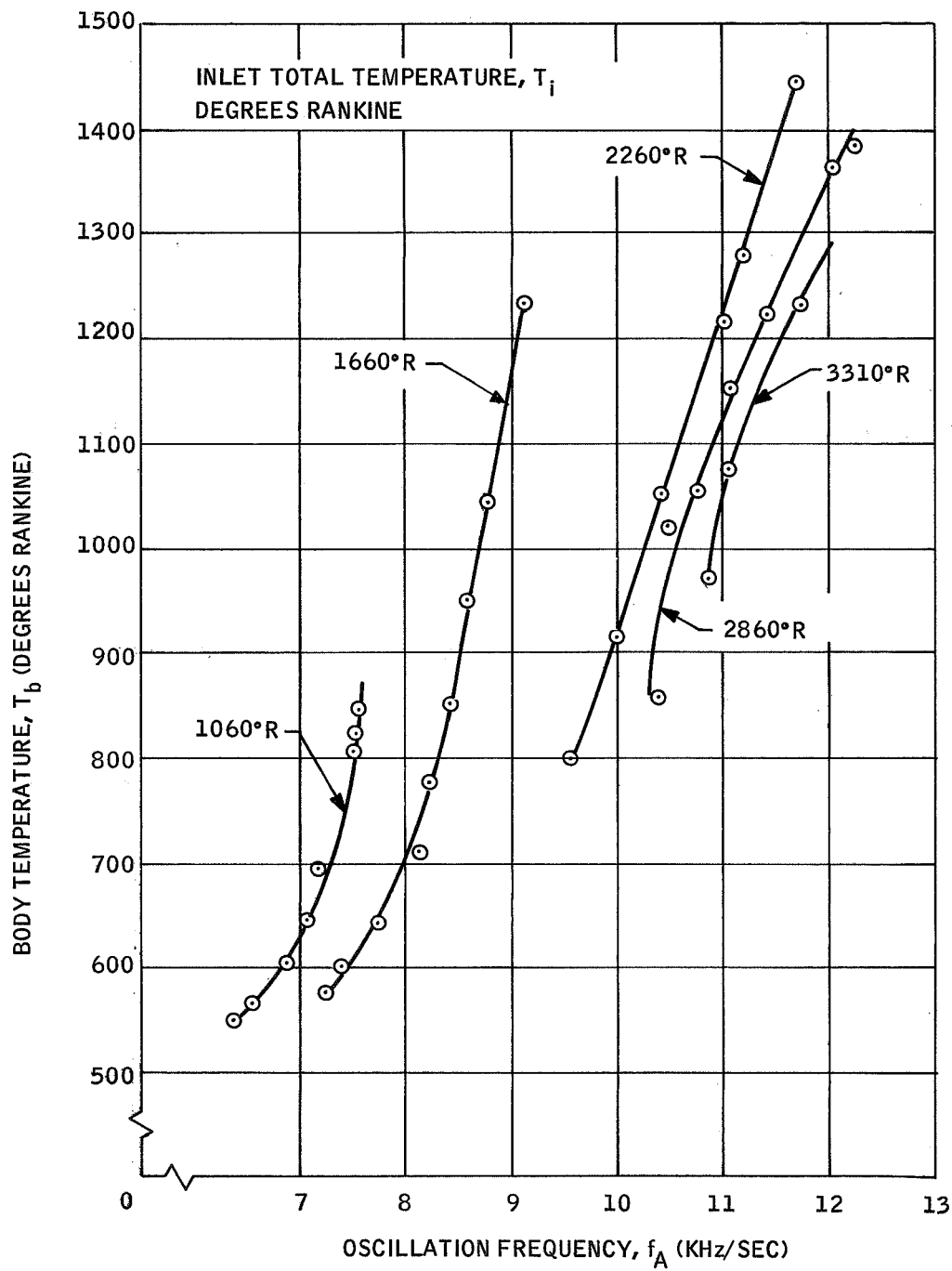


Figure 36. Body Temperature versus Oscillation Frequency for Air, Inlet Total Pressure = 3.0 in. Hg_{ABS}

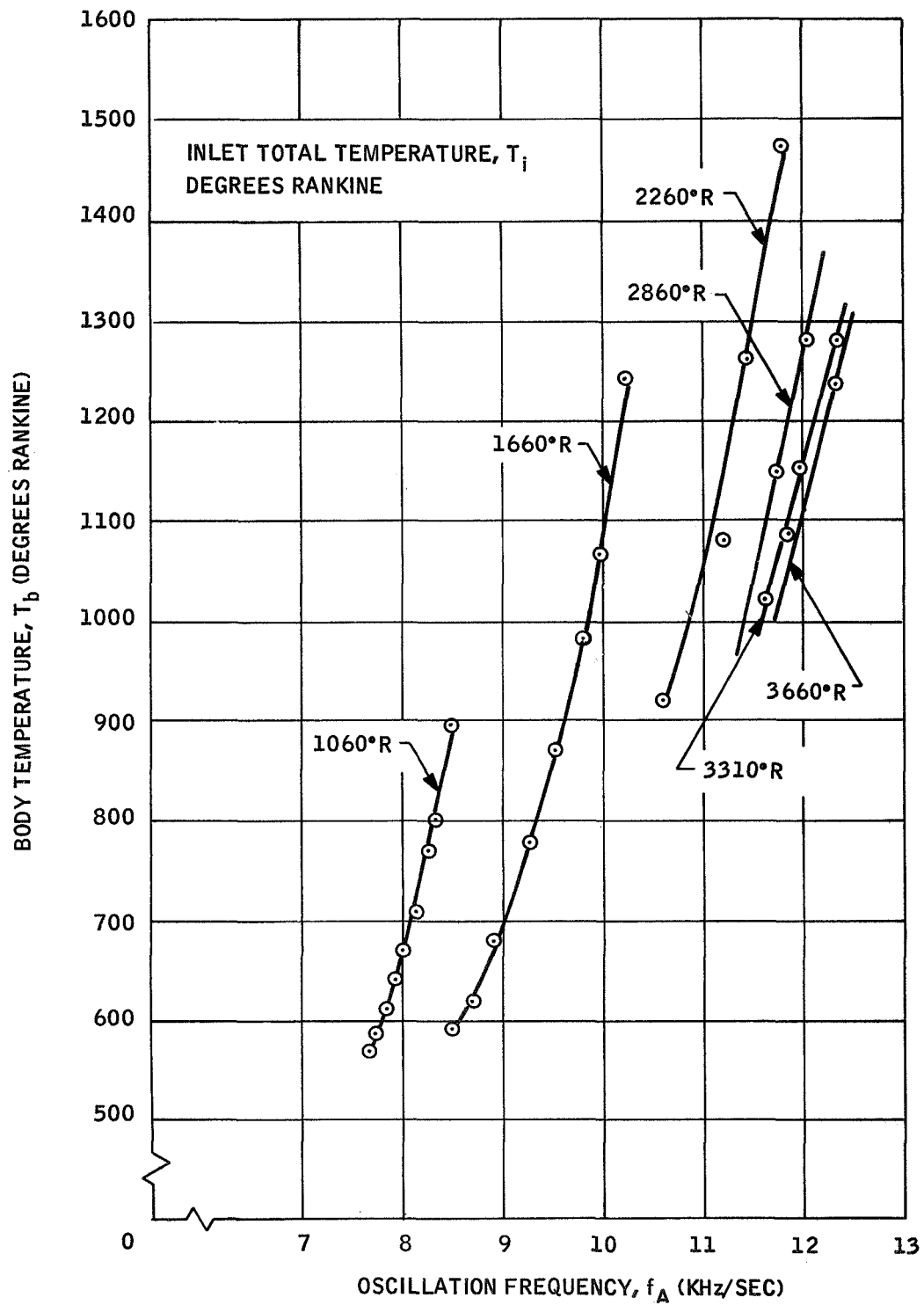


Figure 37. Body Temperature versus Oscillation Frequency for Air, Inlet Total Pressure = 9.0 in. Hg_{ABS}

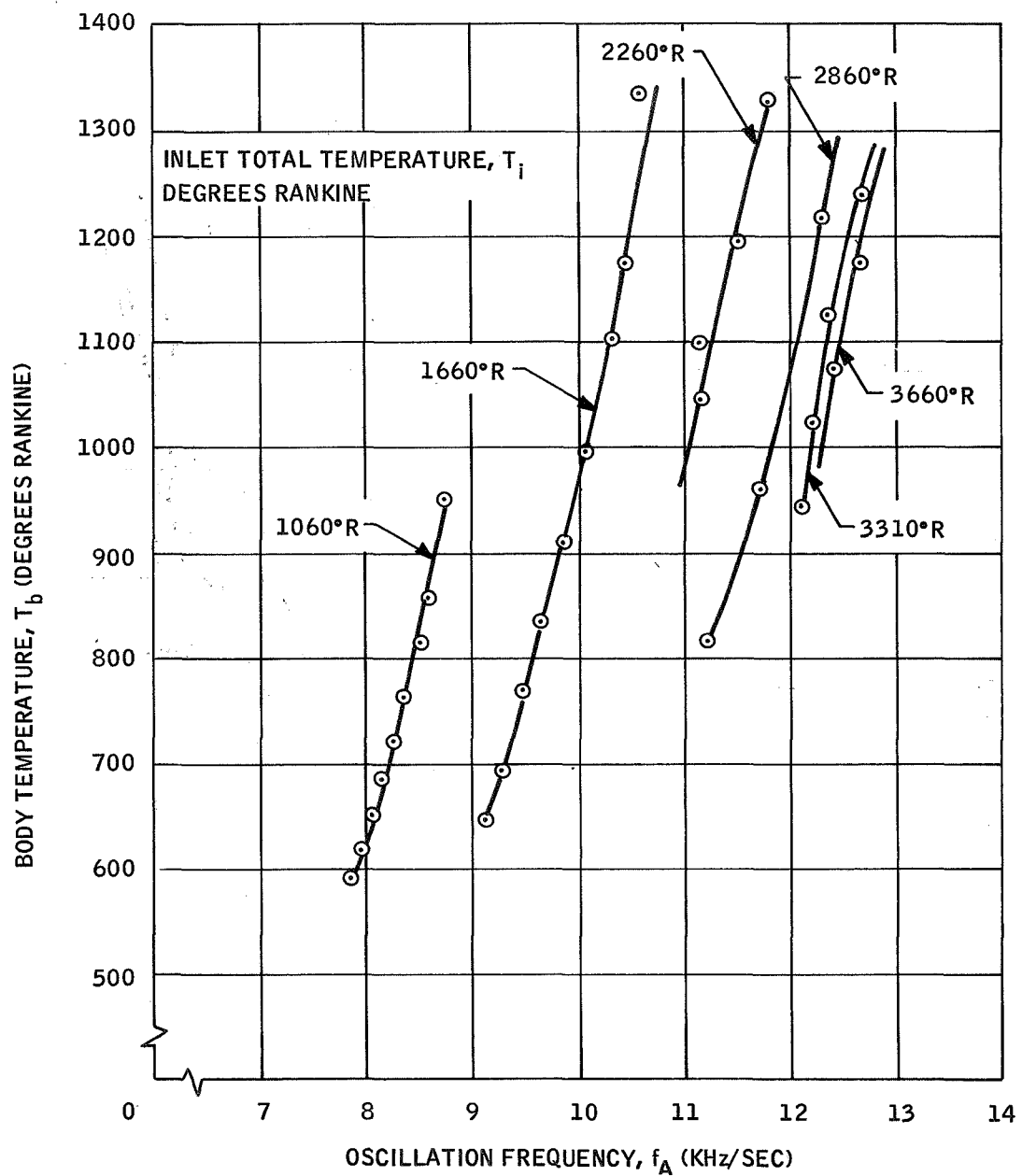


Figure 38. Body Temperature versus Oscillation Frequency for Air, Inlet Total Pressure = 19.0 in. Hg_{ABS}

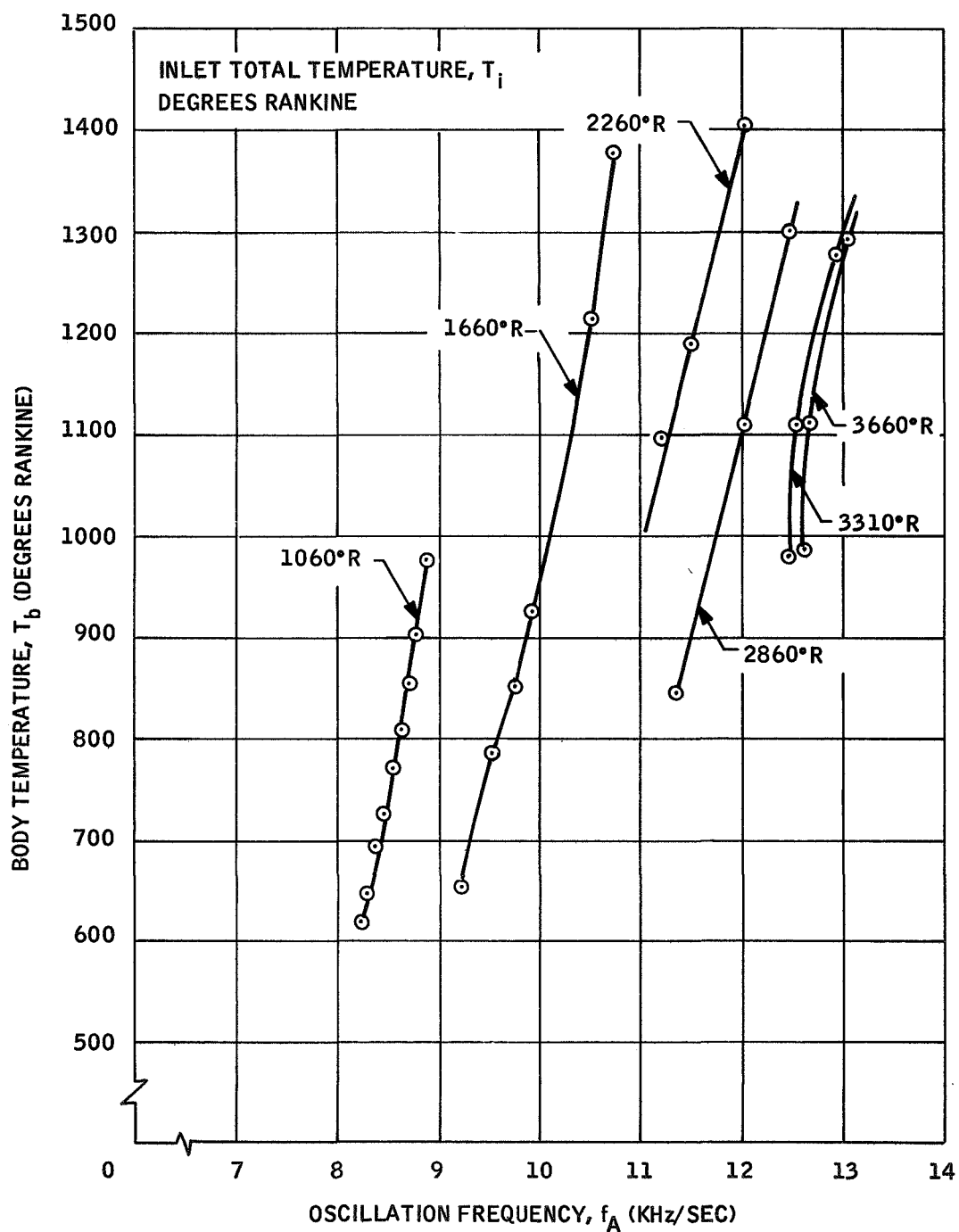


Figure 39. Body Temperature versus Oscillation Frequency for Air, Inlet Total Pressure = 29.0 in. Hg_{ABS}

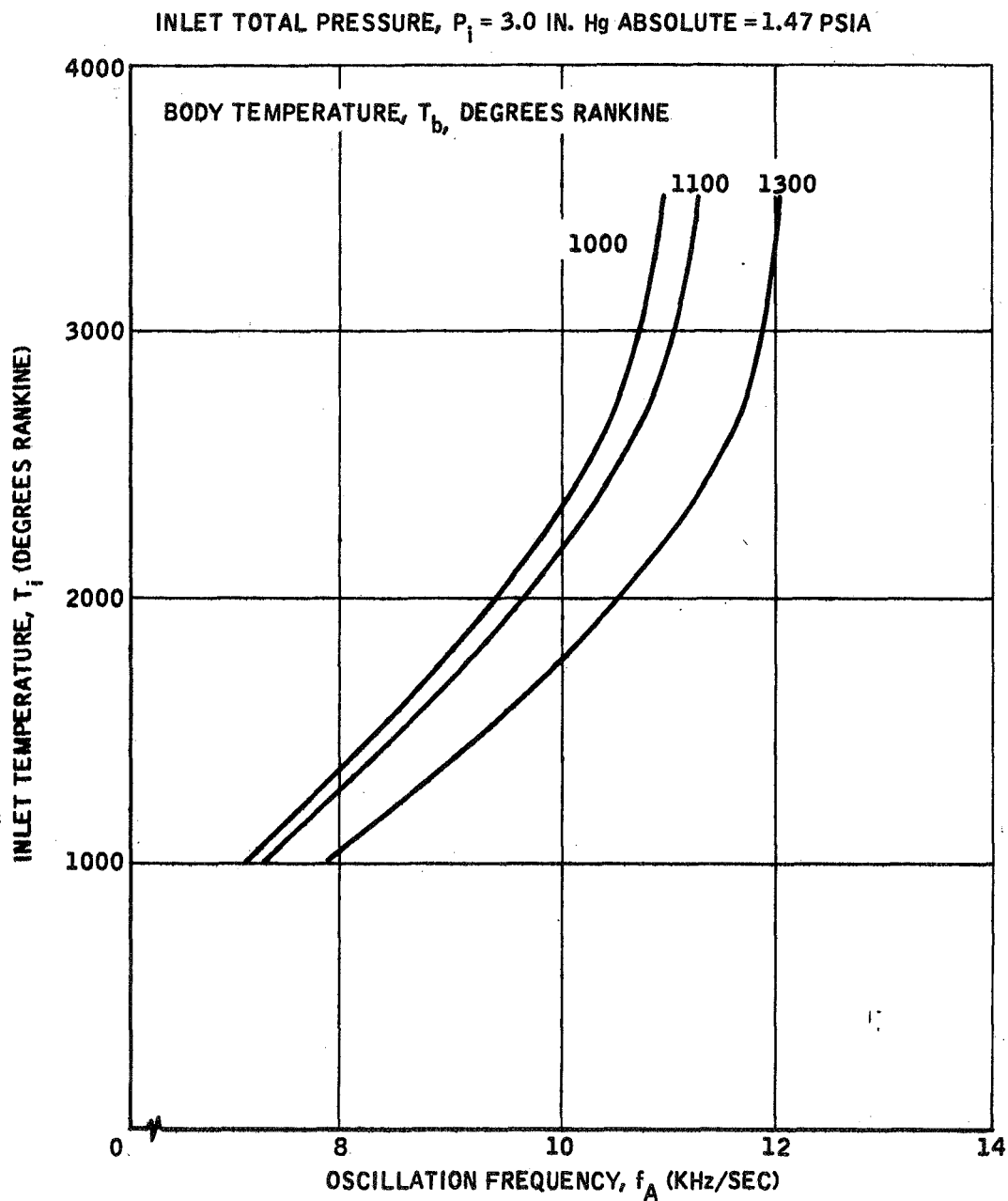


Figure 40. Inlet Temperature versus Oscillation Frequency for Air, Inlet Total Pressure = 3.0 in. Hg_{ABS}

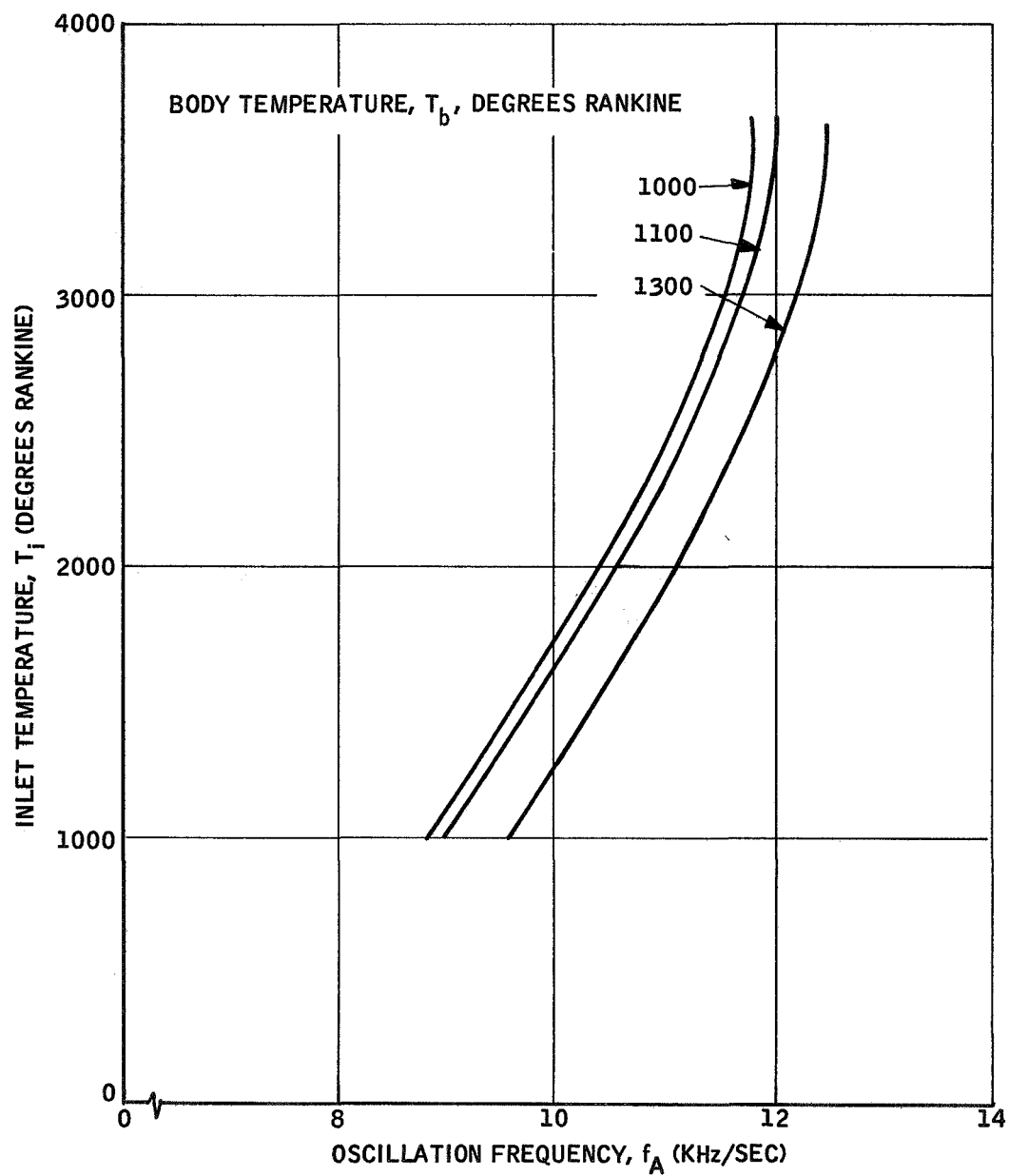


Figure 41. Inlet Temperature versus Oscillation Frequency for Air, Inlet Total Pressure = 9.0 in. Hg_{ABS}

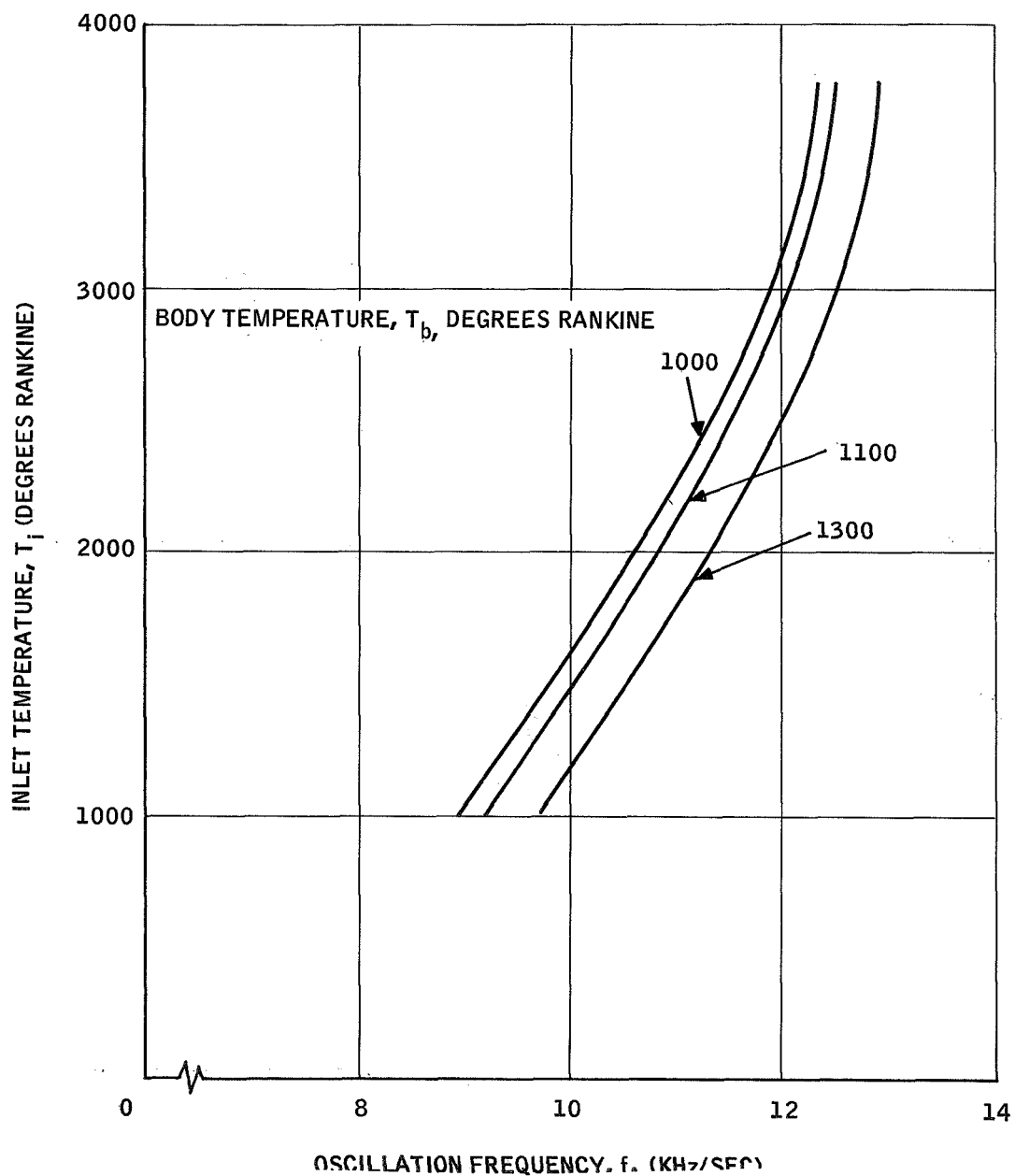


Figure 42. Inlet Temperature versus Oscillation Frequency for Air, Inlet Total Pressure = 19.0 in. Hg_{ABS}

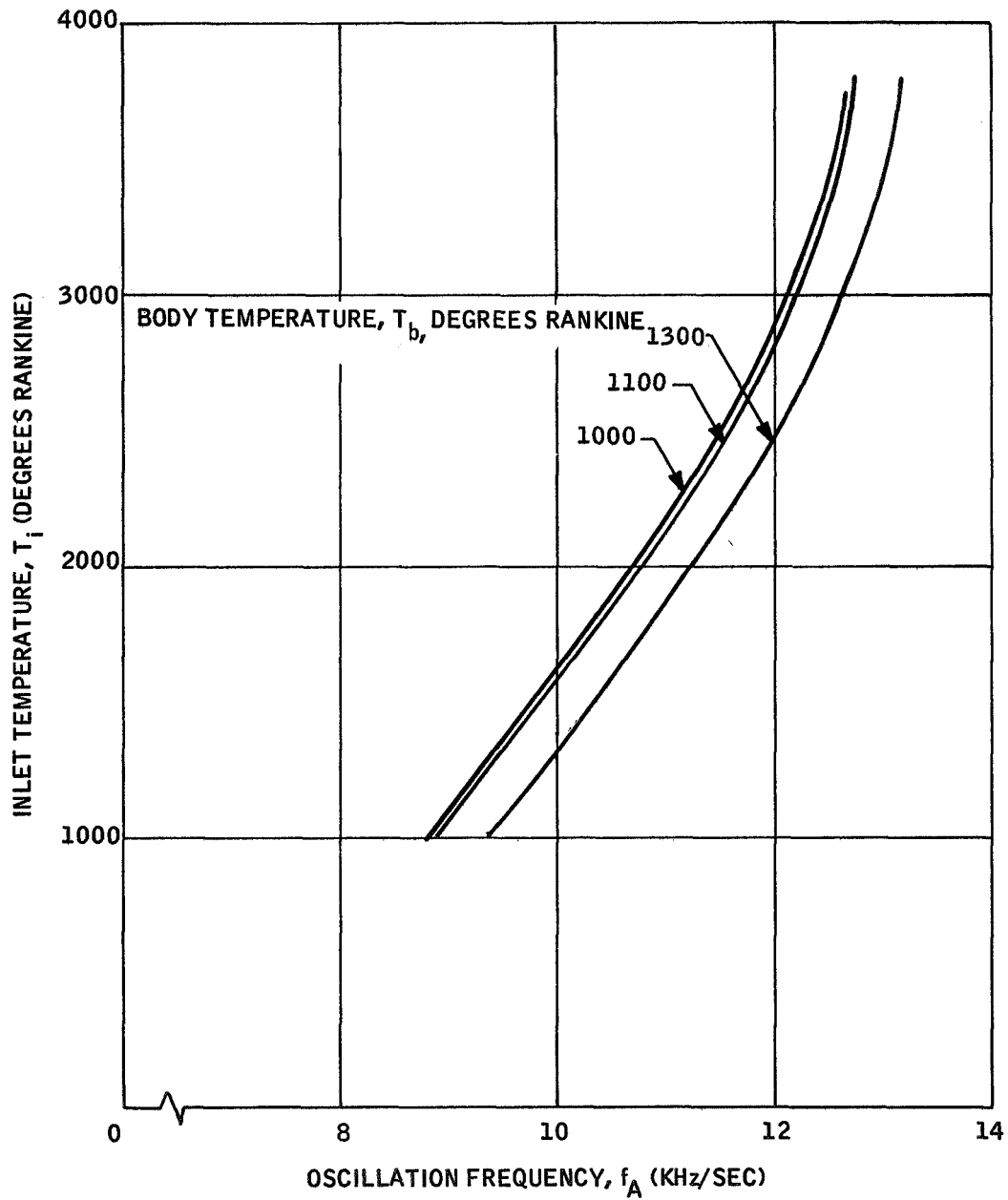


Figure 43. Inlet Temperature versus Oscillation Frequency for Air, Inlet Total Pressure = 29.0 in. Hg_{ABS}

The frequency in air will now be solved as a function of the frequency in nitrogen. The oscillator path length, λ , and the cavity temperature are the same for both air and nitrogen. Also

$$R_A = \frac{\mathcal{R}}{m_A} \text{ and } R_{Ni} = \frac{\mathcal{R}}{m_{Ni}}$$

where

$$m_A = 28.966 \text{ and } m_{Ni} = 28.016$$

As seen in Reference 6, the universal gas constant, \mathcal{R} , varies negligibly with temperature at the pressures involved. Therefore,

$$f_A = 0.9834 f_{Ni} (\gamma_A / \gamma_{Ni})^{0.5}$$

The ratio of specific heats for both air and nitrogen vary as a function of temperature and pressure. In correcting the data, the values for γ_A and γ_{Ni} were taken from Reference 7, Tables of Thermal Properties of Gases.

Additional data for the probes is shown in Figure 44. Sensor oscillation frequency versus inlet total pressure is presented for several cavity temperature values. The frequency dependence on inlet total pressure at room temperature was discussed previously in the SENSOR DESIGN section.

As seen from Figure 44, this independence is also exhibited at high temperature for inlet total pressures ranging from 2.0 psia to 35.0 psia.

Figure 45 is a log-log cross-plot of the data on Figure 44 showing linear relationships between frequency and cavity temperature for the inlet total pressure independent range. Corresponding equations of frequency as a function of cavity temperature and vice versa are noted in the figure.

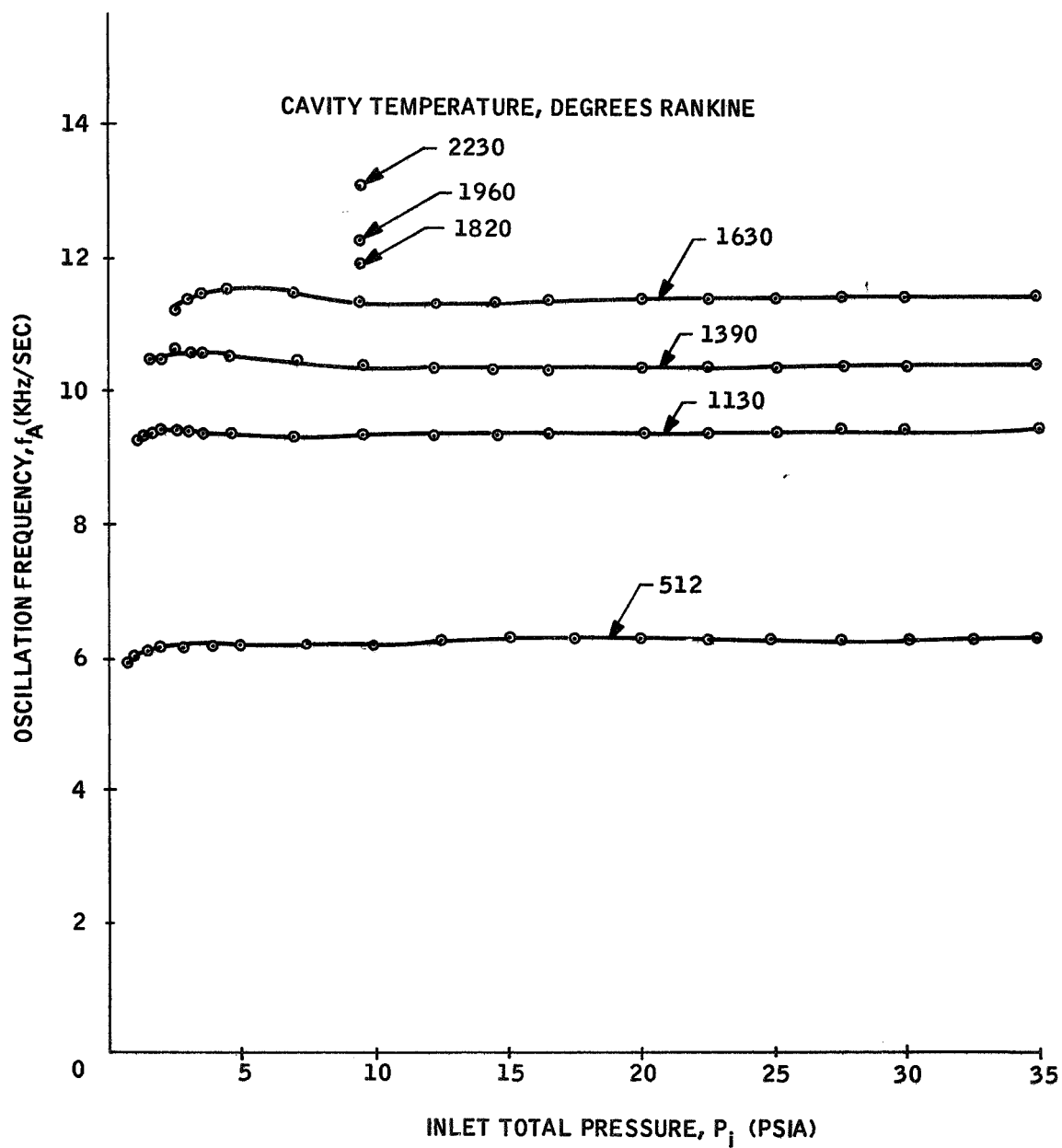


Figure 44. Oscillation Frequency versus Inlet Total Pressure for Air

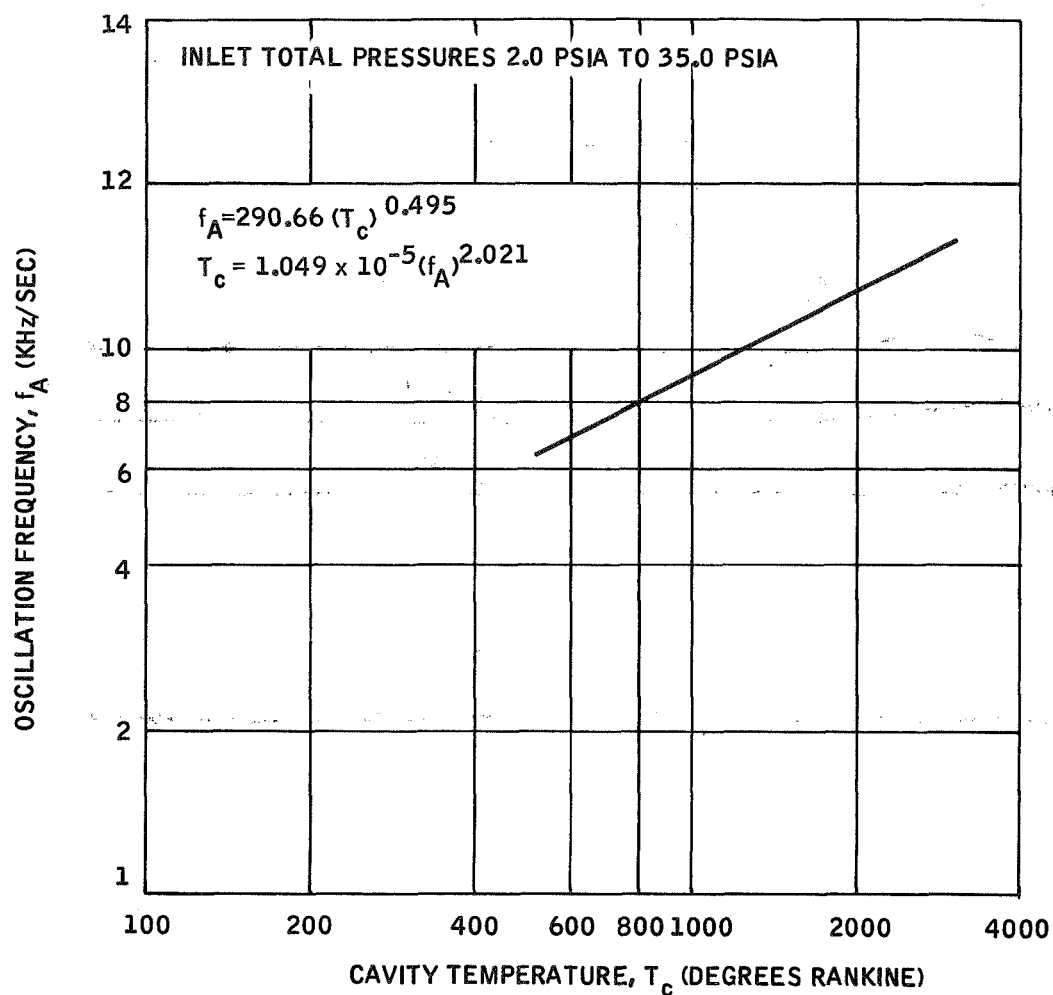


Figure 45. Oscillation Frequency versus Cavity Temperature for Air

A quick check on sensor performance can be made at room temperature. The oscillation frequency should read about 6400 Hz at 535°R (75°F). The check must be made with a vacuum pump which is large enough to produce a flow through the probe such that the exit orifices are choked. At about 535°R and 1 atmosphere inlet pressure, the sensor choked flow rate is about 2.5 scfm.

ENVIRONMENTAL REQUIREMENTS

The fluidic temperature sensor is designed for compatibility with the air-borne environment of X-15 type aerospace vehicles in accordance with the environmental conditions listed below. The conditions apply to the probe and the electronics, converter excepted.

- Temperature:
Probe -- 395°R (-65°F) to the environmental temperature resulting from a total temperature of 5000°R.
Remote signal conditioning -- 395° to 660°R (-65° to 200°F).
- Ambient Pressure: Sea level to 150,000 feet altitude.
- Vibration: 0.06 inch double amplitude from 5 to 55 Hz, ±10 g from 55 to 2000 Hz, each axis.
- Static Acceleration: ±10 g in each axis
- Shock: 50 g for 11±1 millisecond along each axis.
- Radio Interference: The transducer will meet design requirements of Section 3.3 of MIL-I-6181D dated November 25, 1959 with Notice 3 dated June 22, 1965, which ensures that the instrument will neither be affected by nor generate radio frequency interference.

One probe and one electronics package were tested at Honeywell under all of the stated conditions according to the contract Test Plan, Honeywell Document 12080-TP1. The Honeywell evaluation laboratories have the general capability of conforming to and meeting the Military Standard Environmental Test Methods for Aerospace and Ground Equipment, MIL-STD-810 (USAF).

The probe was used to provide a signal to the electronics package during actual testing for all the conditions except static acceleration and shock. Performance checks were made before and after these tests.

The performance of the probe and electronics package was not significantly changed during any of the environmental testing. During the vibration tests, the signal was briefly disturbed as the vibration frequency passed through 1800 Hz. It is felt that 1800 Hz is a resonance point and is of no concern because the sensor signal was very evident and countable at all times.

TESTS ON THE X-15 AIRCRAFT

On 3 October 1967 the X-15 hypersonic aircraft was flown to a new world speed record for winged aircraft of 4534 miles per hour. A Honeywell Inc. developed fluidic temperature sensor, mounted on the X-15 vertical stabilizer during the flight, successfully measured free-stream total temperatures up to about 3300°R. A description of the instrument installation and performance is included in Reference 8.

The sensor that flew with the X-15 had been developed for a similar temperature measuring application for NASA-Ames Research Center hypersonic wind-tunnels. This work was accomplished on NASA Contract NAS7-412, "Study of All-Fluid High Temperature Sensing Probes," the results of which are reported in Reference 3.

A photograph of the miniature probe is shown in Figure 46.

CONCLUSIONS

This document reports the accomplishments of a one-year applied research and development effort conducted by Honeywell Inc., Systems and



Figure 46. Hypersonic Wind Tunnel Fluidic Temperature Probe

Research Center, under NASA Contract NAS4-1211, "High Total Temperature Sensing Probe for the X-15 Hypersonic Aircraft."

The objective of the program was to develop the cooled fluidic oscillator temperature sensor concept into working hardware of a size and design which would be compatible with mounting and operation on high performance aircraft of the X-15 type. The sensor in the form of a probe measures free-stream total temperature.

The probe utilizes the velocity of propagation of an acoustic signal in a cavity to cause oscillatory pressure fluctuations which are related in frequency to the temperature of the operating gas. This frequency, along with the sensor body temperature and local pitot pressure define the probe inlet total temperature. Work accomplished under this contract extended the fluidic temperature sensing technology to accurately measure stagnation temperature up to 5000°R.

Specific areas of accomplishment were:

- Temperature probes were developed which may be operated over a large range of temperature (500°R to 5000°R) and pressure (0.5 psia to 30 psia).
- A cooled fluidic temperature sensor concept was applied to the probe development.
- The probe and associated electronic readout equipment were designed to meet the rigid environmental conditions encountered by high-performance aircraft of the X-15 type.
- The probes were tested and calibrated in the laboratory under simulated flight conditions for inlet temperature and pressure and for typical body temperature profiles.

- The probe was mechanically designed to be compatible with mounting and operation on the X-15 aircraft.

Three stainless steel 446 probes were designed, fabricated, calibrated and delivered to NASA-Flight Research Center along with three sets of associated electronic readout equipment.

REFERENCES

1. Equations, Tables and Charts for Compressible Flow, NACA Report 1135, 1953.
2. Giragosian, P.A., An Empirical Method for the Determination of the Zero-Lift Drag Coefficient of Sharp and Blunt Nosed Conical Exit/Entry Configurations, Space/Planetary Entry Systems Inc., TN 641.
3. Bailey, R. G., et al, A Study of All-Fluid, High-Temperature-Sensing Probes, Honeywell Document 12023-FR1, April 1967, also NASA CR-90092, 1967.
4. Allegheny Ludlum Steel Corporation, Stainless Steel Handbook.
5. Crucible Steel Company of America, Data Book on Stainless Steel, Pipe and Tubing, Titanium, and High Temperature Alloys.
6. Sears, THERMODYNAMICS, Addison-Wesley Publishing Co., Copyright 1953.
7. Hilsenrath, J., et al, Tables of Thermal Properties of Gases, National Bureau of Standards Circular 564, Nov. 1, 1955.
8. Bogue, R. K. and Webb, L.D., NASA Flight Research Center, Advanced Air Data Sensing Techniques, Presented at 5th International Aerospace Instrumentation Symposium, Cranfield, England, March 25-28, 1968.

APPENDIX A

HIGH- AND LOW-TEMPERATURE DATA

This appendix contains tabulated data obtained during the temperature tests described in the body of the report (Temperature Tests and Calibration section).

High-temperature data is contained in Table A1 and low-temperature data in Table A2.

Table A1. High-Temperature Data

T _i (°R)	P _i = 3.0 in. Hg _{ABS} = 1.47 psia					P _i = 9.0 in. Hg _{ABS} = 4.42 psia					P _i = 19.0 in. Hg _{ABS} = 9.34 psia					P _i = 29.0 in. Hg _{ABS} = 14.3 psia				
	f _{Ni} (Hz)	f _A (Hz)	T _C (°R)	T _b (°R)	ċ (scfm)	f _{Ni} (Hz)	f _A (Hz)	T _C (°R)	T _b (°R)	ċ (scfm)	f _{Ni} (Hz)	f _A (Hz)	T _C (°R)	T _b (°R)	ċ (scfm)	f _{Ni} (Hz)	f _A (Hz)	T _C (°R)	T _b (°R)	ċ (scfm)
2260	9740	9561	1160	800	1.21	10800	10601	1410	920	1.21	11350	11141	1575	1100	---	11445	11205	1590	1095	1.08
	10179	9992	1270	915	---	11443	11250	1625	1080	---	11380	11172	1555	1045	---	11720	11504	1660	1188	---
	10700	10503	1445	1040	---	11660	11450	1670	1260	---	11450	11200	1600	1110	---	12250	12025	1830	1405	---
	11390	11210	1600	1280	0.67	12026	11805	1790	1475	---	11700	11510	1690	1195	---					
	11925	11708	1765	1445	---						12000	11779	1775	1330	---					
2860	10700	10479	1420	1020	1.5	12000	11752	1780	1150	1.08	11450	11213	1625	815	4.6	11600	11360	1685	845	---
	10700	10479	1420	1030	1.5	12300	12046	1880	1280	0.81	11750	11510	1690	970	---	12300	12044	1830	1110	2.02
	11300	11066	1590	1152	---						11950	11703	1710	960	2.7	12750	12484	1965	1300	1.08
	12500	12242	1930	1385	---						12560	12298	1885	1220	1.08					
	10600	10381	1405	860	1.35															
3310	11000	10773	1510	1055	0.68															
	11700	11458	1710	1222	0.10															
	12300	12046	1880	1365	0															
	11100	10853	1520	970	2.16	11850	11591	1740	1022	2.30	12400	12101	1890	940	3.65	12750	12477	1995	980	3.50
	11300	11049	1585	1075	1.62	12250	11983	1840	1155	1.67	12500	12199	1925	1022	2.84	12800	12525	2035	1110	2.70
3660	12000	11733	1760	1230	1.08	12600	12325	1960	1280	1.35	12650	12345	1985	1125	2.16	13250	12965	2155	1275	1.63
											13000	12686	2085	1240	1.67					
						12150	11825	1805	1087	2.70	12750	12413	2010	1075	3.10	12900	12610	2030	985	4.32
						12650	12311	1980	1237	1.75	13000	12657	2085	1175	2.56	13000	12657	2095	1110	---
															13400	13046	2225	1292	2.16	

Table A2. Low-Temperature Data

T_i (°R)	$P_i = 3.0 \text{ in. Hg}_{\text{ABS}} = 1.47 \text{ psia}$				$P_i = 9.0 \text{ in. Hg}_{\text{ABS}} = 4.42 \text{ psia}$				$P_i = 19.0 \text{ in. Hg}_{\text{ABS}} = 9.34 \text{ psia}$				$P_i = 29.0 \text{ in. Hg}_{\text{ABS}} = 14.3 \text{ psia}$				$P_i = 39.0 \text{ in. Hg}_{\text{ABS}} = 19.2 \text{ psia}$				$P_i = 49.0 \text{ in. Hg}_{\text{ABS}} = 24.0 \text{ psia}$			
	f_{Ni} (Hz)	f_{A} (Hz)	T_b (°R)	f_{Ni} (Hz)	f_{A} (Hz)	T_b (°R)	f_{Ni} (Hz)	f_{A} (Hz)	T_b (°R)	f_{Ni} (Hz)	f_{A} (Hz)	T_b (°R)	f_{Ni} (Hz)	f_{A} (Hz)	T_b (°R)	f_{Ni} (Hz)	f_{A} (Hz)	T_b (°R)	f_{Ni} (Hz)	f_{A} (Hz)	T_b (°R)	f_{Ni} (Hz)	f_{A} (Hz)	T_b (°R)
1060	7703	7559	844	8646	8484	897	8895	8729	950	9044	8875	976	9173	9002	970	9238	9066	986	9157	8887	915	9118	8949	890
	7675	7531	826	8506	8347	802	8751	8591	857	8960	8793	900	9061	8892	895	9157	8887	915	9118	8949	890	9118	8949	890
	7634	7491	807	8450	8292	770	8655	8495	815	8894	8728	855	9010	8842	865	9118	8842	890	9118	8949	890	9118	8949	890
	--	--	755	8300	8145	709	8525	8366	762	8820	8656	810	8935	8769	823	9041	8873	--	9041	8873	--	9041	8873	--
	7315	7178	695	8175	8022	670	8424	8267	722	8735	8572	770	8847	8682	801	8972	8805	812	8972	8805	812	8972	8805	812
	7206	7071	645	8109	7957	640	8316	8161	685	8638	8477	725	8765	8602	767	8896	8730	787	8896	8730	787	8896	8730	787
	7000	6869	604	8000	7850	612	8218	8064	652	8548	8389	692	8690	8528	732	8835	8671	755	8835	8671	755	8835	8671	755
	6857	6722	584	7887	7740	587	8097	7946	617	8453	8295	645	8592	8432	683	8806	8642	707	8806	8642	707	8806	8642	707
	6490	6369	549	7805	7659	569	8020	7870	592	8400	8243	618	8546	8387	635	8738	8576	652	8738	8576	652	8738	8576	652
1660	9285	9123	1232	10400	10219	1240	10846	10657	1337	10936	10748	1390	10992	10803	1307	11269	11075	1395	11269	11075	1395	11269	11075	1395
	8950	8794	1042	10140	9964	1067	10610	10426	1175	10716	10532	1215	10865	10678	1235	11238	11045	1355	11238	11045	1355	11238	11045	1355
	8732	8580	952	9972	9799	980	10480	10298	1107	10595	10412	1142	10648	10465	1115	11172	10980	1290	11172	10980	1290	11172	10980	1290
	8576	8427	852	9693	9524	870	10234	10056	995	10398	10218	1040	10473	10293	1010	11106	10915	1210	11106	10915	1210	11106	10915	1210
	8365	8219	777	9435	9271	790	10023	9849	910	10117	9943	925	10283	10106	925	11038	10848	1125	11038	10848	1125	11038	10848	1125
	8258	8115	716	9077	8919	680	9811	9641	834	9947	9775	850	10154	9979	857	10979	10790	1045	10979	10790	1045	10979	10790	1045
	7886	7749	642	8861	8707	620	9641	9473	770	9713	9546	784	9995	9823	764	10877	10690	945	10877	10690	945	10877	10690	945
	7513	7382	602	8658	8507	590	9432	9268	695	9521	9357	--	9955	9784	667	10780	10595	860	10780	10595	860	10780	10595	860
	7363	7235	576				9286	9125	645	9385	9224	657												

APPENDIX B
ELECTRONIC COMPONENT SPECIFICATIONS

PRESSURE TRANSDUCER
KISTLER Model 601R

Pressure range	10 to 3000 psi
Resolution	0.1 psi
Maximum pressure	5000 psi
Sensitivity (nominal)	1 picocoulomb/psi
Resonant frequency (mounted)(nominal)	130,000 Hz
Rise time	3 microseconds
Linearity	1 percent
Capacitance (nominal)	5 picofarads
Insulation resistance (minimum)	10^{14} ohms
Acceleration sensitivity	0.01 psi/g
Temperature sensitivity	0.01 percent /°R
Temperature range	0 to 1500°R
Intermittent gas temperature on diaphragm	> 3500°R
Shock and vibration	15,000 g's
Cable connector	Kistler 4mm
Mounting thread with connector adaptor	7 x 0.75mm
Sensing element	crystalline quartz
Case material: body; diaphragm	430F SS; 316 SS
Size	0.25 x 0.6 inch
Weight (approximate)	0.08 oz., 2.25 gm

DUAL REGULATED MODULAR POWER SUPPLY
BURR-BROWN Model 501

Supply voltage	105 to 125 v rms
Supply frequency	50 to 420 Hz
Supply drain	10 volt-amperes
Output voltage	± 15 vdc
Voltage accuracy	± 1 percent
Rated output current	0 to ± 100
Short circuit current	± 250 ma
Output noise	0.6 ma
Module size	3.4 x 2.9 x 1.9 inches
Module weight	2.5 pounds, nominal

OPERATIONAL AMPLIFIER
ANALOG DEVICES Model 183C

Open loop gain, dc rated load, min.	2×10^5 vdc
Rated output, voltage, min.	± 10 v
Rated output, current, min.	5 ma
Frequency response, unity gains	0.5 MHz
Input impedance, differential	2 m ohms
Input voltage range, common mode voltage, min.	± 10 v
Temperature range	385 to 645°R
Size, overall	1.5 x 0.6 x 1.5 inches

FREQUENCY-TO-VOLTAGE CONVERTER

MATRIX 1210 Series

Input frequency (independent of waveform)	0-100 KHz, for full scale output
Input voltage	±1 volt p-p, to 240 volts p-p
Input resistance	100,000 ohms
Output wave form	Positive pulse with amplitude of 10 volts, width approx. one-half period of full scale frequency
Output impedance	5,000 ohms
Response time	One period of the operating frequency
Linearity	±0.1% of full scale from best zero-based straight line
Drift	±0.07% of full scale for 24 hours after 1-hour warm up
Temperature coefficient	±0.01% per degree R (492 to 582°R)
Temperature	Operating 492 to 582°R, storage 330 to 628°R
Line voltage stability	±1.0% of full scale for + 10% line change
Power	+ 24 vdc at 30 ma
Connector supplied	10-pin P.C. -type
Dimensions	2 1/2 in. high, 2 1/4 in. wide, 3/4 in. thick